[redacted]

PRINCETON UNIVERSITY

DEPARTMENT OF

AEROSPACE AND MECHANICAL SCIENCES

National Aeronautics and Space Administration
NGL 31-001-005

PULSED ELECTROMAGNETIC GAS ACCELERATION

1 January 1971 to 30 June 1971

Semi-annual Report 634q

Prepared by: Robert G. Jahn
Robert G. Jahn
Dean of Engineering and
Principal Investigator

and

Woldemar v. Jaskowsky
Woldemar F. von Jaskowsky
Sr. Research Engineer and
Lecturer

Kenn E. Clark
Kenn E. Clark
Research Staff Member

July 1971

School of Engineering and Applied Science
Department of Aerospace and Mechanical Sciences
Guggenheim Aerospace Propulsion Laboratories
PRINCETON UNIVERSITY
Princeton, N.J.08540

ABSTRACT

Experimental data are combined with one-dimensional conservation relations to yield information on the energy deposition ratio in a parallel-plate accelerator, where the downstream flow is confined to a constant area channel. Approximately 70% of the total input power is detected in the exhaust flow, of which only about 20% appears as directed kinetic energy, thus implying that a downstream expansion to convert chamber enthalpy into kinetic energy must be an important aspect of conventional high power MPD arcs.

Spectroscopic experiments on a quasi-steady MPD argon accelerator verify the presence of AIII and the absence of AI, and indicate an azimuthal structure in the jet related to the mass injection locations. Measurements of pressure in the arc chamber and impact pressure in the exhaust jet using a piezocrystal backed by a Plexiglas rod are in good agreement with the electromagnetic thrust model.

Other experiments related to various aspects of MPD accelerator operation continue: additional characteristics of a hollow-cathode MPD arc are determined; first indications of thrust-time profiles are obtained; a study is initiated on the biased double probe in the exhaust plasma; and mass pulses are recorded from a new turbo-injector device.

CONTENTS

LIST OF ILLUSTRATIONS

LIST OF TABLES

CURRENT STUDENT PARTICIPATION

Student	Period	Degree	Thesis Topic
BOYLE, Michael J.	1968-1969 1971	Ph.D. Cand.	Velocity and Acceleration Patterns in the MPD Exhaust
BRUCKNER, Adam P.	1966-	Ph.D. Cand.	Time-Resolved Spectroscopy of the MPD Exhaust Plume
CORY, John S.	1969-	Ph.D. Cand.	Mass, Momentum and Energy Flow from an MPD Accelerator
DI CAPUA, Marco S.	1966-	Ph.D. Cand.	Energy Deposition in Parallel-Plate Plasma Accelerators
FOURNIER, Georges	1969-71	B.S.E.	Optical Spectroscopy of Accelerator Exhaust Flow
HIXON, Todd L.	1970-	A.B. Cand.	Spectroscopic-Interferometric Studies of MPD Discharge Plasmas
HOUGH, Michael E.	1969-1971	B.S.E.	Mass Spectrometry of Accelerator Exhaust Flow
PARMENTIER, Noël	1970-	M.S.E. Cand.	Quasi-Steady MPD Arc with Hollow Cathode
SABER, Aaron J.	1969-	Ph.D. Cand.	Thrust Measurements on Quasi-Steady Accelerators
VILLANI, Daniel D.	1969-	Ph.D. Cand.	MPD Discharge Studies with Solenoid Valve Injection System
WHITE, Fred W.	1969-	M.S.E. Cand.	Propellant Injection Techniques for Quasi-Steady Accelerators

I. INTRODUCTION

This semi-annual report contains a review of a Ph.D. research program recently completed in our laboratory, along with more concise descriptions of several other programs presently in progress. The first section outlines the use of a variety of experimental results in a one-dimensional model to determine the energy deposition ratio in our parallel-plate accelerator, a major portion of the Ph.D. thesis of M. S. DiCapua. In the second section, results from various studies on the pulsed MPD accelerator are presented, including velocity and species data based on both time-resolved and time-integrated spectroscopic techniques and the use of a piezoelectric pressure probe to determine the chamber pressure and impact pressure profile in the exhaust. The final section reviews the progress of other programs in various stages of completion from preliminary and feasibility tests to well established areas of research. These include terminal data on an MPD arc with a hollow cathode whose outer surface is insulated, further progress with the time-resolved thrust measurement technique, a study to determine the applicability of the biased double-probe as a diagnostic tool in the MPD exhaust, and the first tailored mass pulses generated with the turbo-pulse gas injector. More detailed reports on these programs, as well as on other studies in progress will be deferred until the following report.

II. ENERGY DEPOSITION IN THE PARALLEL-PLATE PLASMA ACCELERATOR (DiCapua)

A. Introduction

The central interest of this study is the initial apportionment of the input power to the streaming and thermal energy of the flow in a plasma accelerator. This initial energy deposition ratio achieves great importance if one is committed to the task of efficient plasma acceleration. Insufficient detailed knowledge of the electromagnetic, gasdynamic, and thermodynamic fields throughout the acceleration region commits us to obtain the energy deposition ratio through a black box or terminal analysis of the accelerator. This analysis is based upon measurement of the terminal electrical parameters of the accelerator and upon observation of properties of the flow into and out of the acceleration region. A self-consistent picture can then be drawn through the application of momentum and energy conservation arguments. Even on this basis, however, several complications arise due to the complex non-equilibrium state of the working fluid and the introduction of spurious mass into the flow through electrode and insulator erosion as well as ingestion of mass associated with the gasdynamic flow field established prior to the initiation of the discharge.

The parallel plate geometry is particularly well suited for this analysis. The electromagnetic fields upstream of the acceleration zone can be obtained through simple one dimensional arguments. Downstream of the acceleration zone, the plasma flow field is amenable to a steady, one-dimensional treatment as well. The first task, therefore, is to obtain the conservation relations in a convenient form for the analysis.

B. The Conservation Relations

Analysis of the problem in a terminal fashion can best be performed with the conservation relations cast in integral

form. This approach allows treatment on the basis of mass, momentum, and energy fluxes across appropriate surfaces without requiring any detailed knowledge of the processes which occur within the acceleration region.

1. Mass Conservation

The mass conservation equation for an arbitrary fixed volume can be written as:[II-1]

$$\int_V \frac{\partial \rho}{\partial t} dV = - \oint_A \rho \vec{u} \cdot d\vec{A} \qquad (1)$$

where ρ is the density, $\vec{u}$, the velocity, V, the total volume, A, the total surface area of that volume, and dV and dA are respectively the volume and surface elements.

2. Momentum Conservation

The momentum conservation equation in integral form can be written as:[II-1]

$$\int_V \frac{\partial}{\partial t}(\rho \vec{u}) dV + \oint_A \rho \vec{u} (\vec{u} \cdot d\vec{A}) = - \oint_A p \, dA + \int_V \vec{f} \, dV + \oint_A \vec{\tau} \cdot d\vec{A} \qquad (2)$$

where p is the pressure, $\vec{f}$, the body force per unit volume, and $\vec{\tau}$, the viscous stress tensor. In this case, where electromagnetic forces are present, $\vec{f}$ takes the form:

$$\vec{f} = \vec{j} \times \vec{B} \qquad (3)$$

where $\vec{j}$ is the current density and $\vec{B}$ is the magnetic field.

To transform the volume integral of the body forces into the required surface integral, the body force must be cast in the form of the divergence of a tensor.[II-2] The tensor can then be integrated over the surface. To this end, the body force becomes:

$$\vec{f} = \vec{j} \times \vec{B} = \frac{1}{\mu_o} (\nabla \times \vec{B}) \times \vec{B} \qquad (4)$$

through the use of Ampere's Law in the low frequency limit:

$$\nabla \times \vec{B} = \mu_o \vec{j} \qquad (5)$$

Using the vector identity:

$$(\nabla \times \vec{B}) \times \vec{B} = (\vec{B} \cdot \nabla)\vec{B} - \frac{1}{2}\nabla(\vec{B}\cdot\vec{B}) \tag{6}$$

with:

$$0 = \vec{B}(\nabla \cdot \vec{B}) \tag{7}$$

added to both sides, the body force becomes:

$$\vec{f} \times \vec{B} = \frac{1}{\mu_o}(\nabla \times \vec{B}) \times \vec{B} = \nabla \cdot \frac{1}{\mu_o}\left(\vec{B}\vec{B} - \frac{1}{2}\vec{\vec{I}}B^2\right) \tag{8}$$

where

$$B^2 = \vec{B}\cdot\vec{B}$$

$$\text{and} \quad \vec{\vec{I}} = \delta_{ij} \tag{9}$$

The right hand term of equation (8) is the divergence of that part of the Maxwell stress tensor which is associated with the magnetic field.

By Gauss's theorem the volume integral is transformed into the desired surface integral:

$$\int_V \vec{f}\, dV = \frac{1}{\mu_o}\oint_A \vec{B}(\vec{B}\cdot d\vec{A}) - \frac{1}{2\mu_o}\oint_A B^2 d\vec{A} \tag{10}$$

and the momentum equation becomes:

$$\int_V \frac{\partial}{\partial t}(\rho\vec{u})\, dV + \oint_A \rho\vec{u}(\vec{u}\cdot d\vec{A}) = -\oint_A\left(p + \frac{B^2}{2\mu_o}\right)d\vec{A} + \oint_A \frac{\vec{B}}{\mu_o}(\vec{B}\cdot d\vec{A}) + \oint_A \vec{\vec{\tau}}\cdot d\vec{A} \tag{11}$$

3. Energy Conservation

The energy conservation equation in integral form is:[II-1]

$$\int_V \frac{\partial}{\partial t}\left[\rho\left(e + \frac{u^2}{2}\right)\right] dV + \oint_A \rho\left(e + \frac{u^2}{2}\right)\vec{u}\cdot d\vec{A} = -\oint_A p\vec{u}\cdot d\vec{A}$$

$$+\oint_A (\vec{u}\cdot\vec{\vec{\tau}})\cdot d\vec{A} + \int_V \left(\frac{\partial}{\partial t}\frac{B^2}{2\mu_o} + \vec{j}\cdot\vec{E}\right)dV + \oint_A \vec{q}\cdot d\vec{A} \tag{12}$$

where e is the internal energy per unit mass, $\frac{\partial}{\partial t}\frac{B^2}{2\mu_o}$ is the time rate of change of energy per unit volume associated with the magnetic field, and $\vec{q}$ is the heat flux vector. The quantity $\vec{j}\cdot\vec{E}$ where $\vec{j}$ is the current density as before and $\vec{E}$ is the electric field, represents the rate of conversion of electromagnetic field energy into mechanical and thermal modes.

It is again advantageous to transform the volume integrals associated with the electromagnetic fields into surface integrals which are more closely related to the terminal parameters of the accelerator. To this end, using Ampere's Law:

$$\frac{\partial}{\partial t}\frac{B^2}{2\mu_o} + \vec{j}\cdot\vec{E} = \frac{\partial}{\partial t}\frac{B^2}{2\mu_o} + \frac{\nabla\times\vec{B}}{\mu_o}\cdot\vec{E} \tag{13}$$

With the identity:

$$(\nabla\times\vec{E})\cdot\vec{B} - \vec{E}\cdot(\nabla\times\vec{B}) = \nabla\cdot(\vec{E}\times\vec{B}) \tag{14}$$

and Faraday's Law:

$$\nabla\times\vec{E} = -\frac{\partial\vec{B}}{\partial t} \tag{15}$$

equation (13) becomes:

$$\frac{\partial}{\partial t}\frac{B^2}{2\mu_o} + \vec{j}\cdot\vec{E} = -\nabla\cdot(\vec{E}\times\vec{B}) \tag{16}$$

Thus, using Gauss's theorem,

$$\int_V \left(\frac{\partial}{\partial t}\frac{B^2}{2\mu_o} + \vec{j}\cdot\vec{E}\right)dV = -\oint_A \frac{(\vec{E}\times\vec{B})}{\mu_o}\cdot d\vec{A} \tag{17}$$

The term $\frac{\vec{E}\times\vec{B}}{\mu_o}$ is the Poynting vector which represents the flux per unit area per unit time of electromagnetic energy. The energy equation therefore takes the form:

$$\int_V \frac{\partial}{\partial t}\left[\rho\left(e+\frac{u^2}{2}\right)\right]dV + \oint_A \rho\left(h+\frac{u^2}{2}\right)\vec{u}\cdot d\vec{A} = -\oint_A \frac{(\vec{E}\times\vec{B})}{\mu_o}\cdot d\vec{A}$$

$$+\oint_A (\vec{u}\cdot\vec{\tau})\cdot d\vec{A} + \oint_A \vec{q}\cdot d\vec{A} \tag{18}$$

where the enthalpy h is defined as:

$$h = e + p/\rho \tag{19}$$

C. The Steady One-Dimensional Approach

The conservation relations derived in the previous section can be greatly simplified under the assumption of steady one-dimensional flow. With this assumption all terms containing time derivatives vanish and all properties of the flow and the electromagnetic field become the function of only one

coordinate, namely the x coordinate as shown in Fig. II-1. The relations are further simplified with the assumption of negligible viscous and heat transfer effects to be justified later.

The geometry of the accelerator is shown schematically in Fig.II-1. The channel has an area A of width w and height h. The injector orifices in the back wall have a total area A_1. The injected argon propellant has a pressure at the exit plane of the orifices of p_1, a density ρ_1, and a velocity u_1 in the x direction. A current J flows through the backstrap and accelerator causing a voltage drop across the electrodes of V. Downstream of the acceleration region the pressure is p, the density ρ, and the velocity u in the x direction.

Under the steady, one-dimensional assumption, the electromagnetic fields are obtained from the current and voltage across the accelerator. Although the voltage drop across the terminals is V, only a portion of this is imposed upon the plasma flow due to the anode and cathode fall voltages. An empirical correction factor α is used to denote that fraction, i.e α V J represents the fraction of the total input power available to the flow. It follows that the electric field everywhere within the plasma except in the falls can be determined from

$$\int \vec{E}_1 \cdot d\vec{\ell} = \alpha V \tag{20}$$

from which

$$\vec{E}_1 = -\frac{\alpha V}{h}\,\hat{e}_y \tag{21}$$

assuming E_1, the electric field as defined above, is constant along the height. By Ampere's Law, on the other hand,

$$\oint \vec{B} \cdot d\vec{\ell} = \mu_0 J \tag{22}$$

and therefore the magnetic field B_1 is:

$$\vec{B}_1 = -\frac{\mu_0 J}{w}\,\hat{e}_z \tag{23}$$

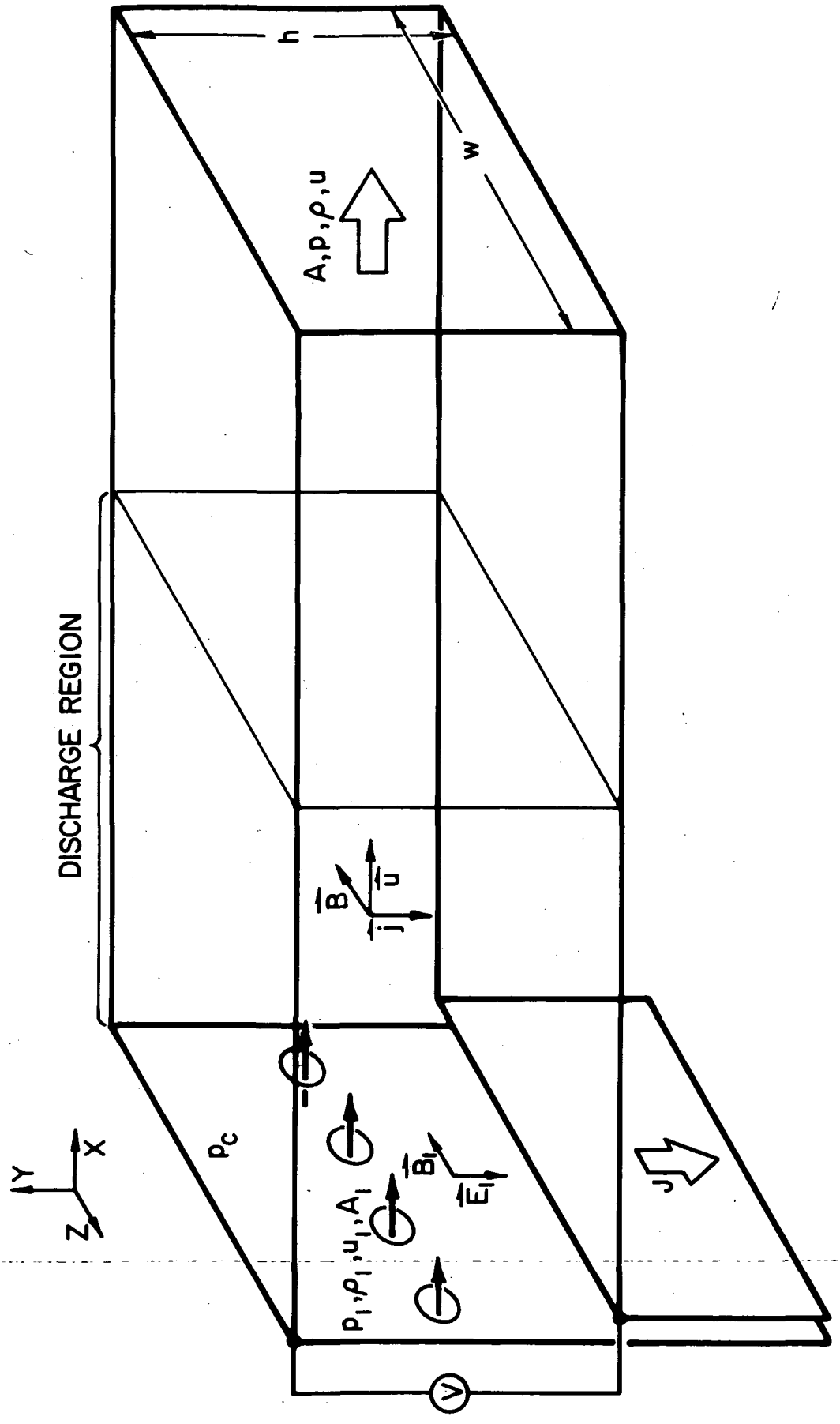

SCHEMATIC OF PARALLEL PLATE ACCELERATOR

FIGURE II-1
AP25-4730

The Conservation relations therefore become:

$$\rho_1 u_1 A_1 = \rho u A \qquad \text{Mass} \qquad (24)$$

$$\rho u^2 A - \rho_1 u_1^2 A_1 = p_1 A_1 + A\left(p_c - p + \frac{\mu_0 J^2}{2w^2}\right) \qquad \text{Momentum} \qquad (25)$$

$$\rho u A\left(h + \frac{u^2}{2}\right) - \rho_1 u_1 A_1\left(h_1 + \frac{u_1^2}{2}\right) = \alpha V J \qquad \text{Energy} \qquad (26)$$

D. Experimental Results

The experimental data strongly suggest that the steady analysis is applicable to this accelerator. A typical simultaneous record of current J, terminal voltage V and inductive voltage V_D taken at the 85 kA, 96g/sec operating condition is shown in Fig.II-2a.The current rises in 10 μsec and remains constant for 180 μsec. The inductive voltage, which is associated with changes of magnetic flux in the accelerator due to time derivatives of the total current or motion of the current distribution, drops to a negligible value after 50 μsec and remains practically zero until 180 μsec when the current begins to drop. The voltage V, which is measured downstream of the current distribution, represents the sum of the resistive voltage and the induced emf across the accelerator. This voltage assumes a constant value after 50 μsec and begins to drop at 180 μsec, indicating steady electrodynamic operation of the accelerator in this time interval.

Measurements of pressure in the accelerator channel show that steady gasdynamic operation is achieved as well. Fig.II-2b shows triple overlays of simultaneous pressure measurements taken 10 cm upstream of the electrode insulator junction and 23 cm downstream of the junction in the centerline of the channel top. The peak in the upstream pressure p_c is associated with the unsteady phase of the discharge. The second and third peaks are due to internal reflections in the probe so that the upstream pressure achieves a low but steady value of about 0.03 atm roughly at the same time the voltage reaches the steady phase.

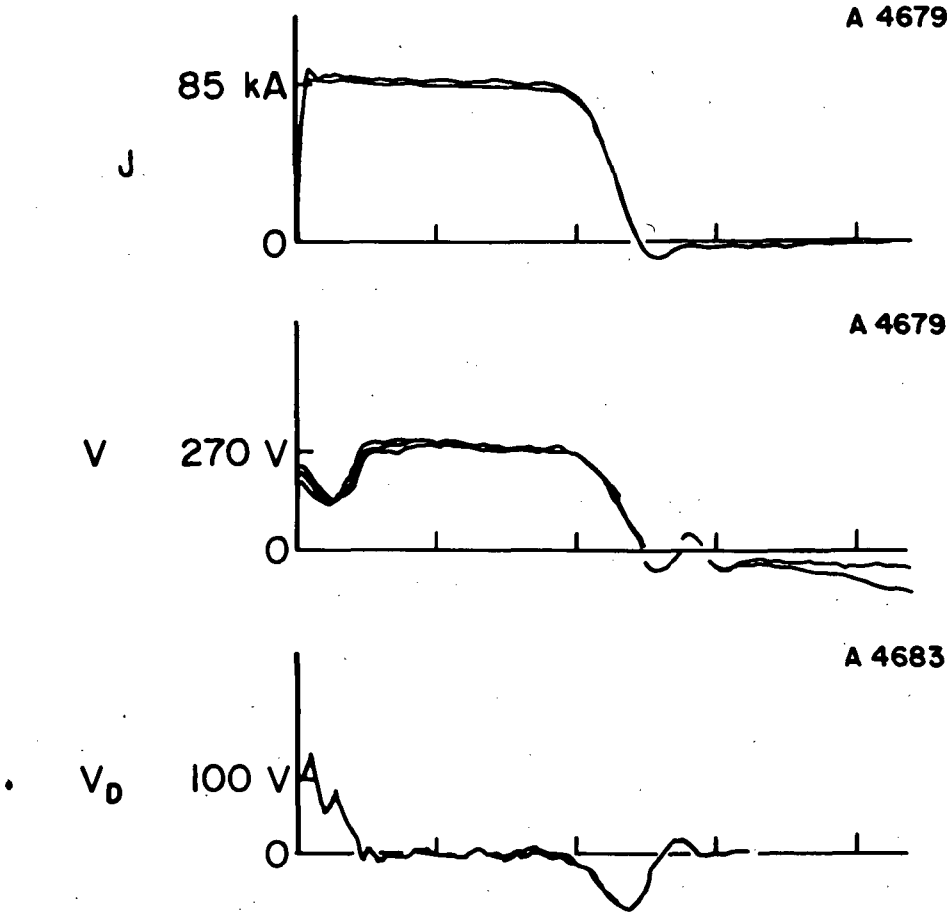

a) TERMINAL MEASUREMENTS

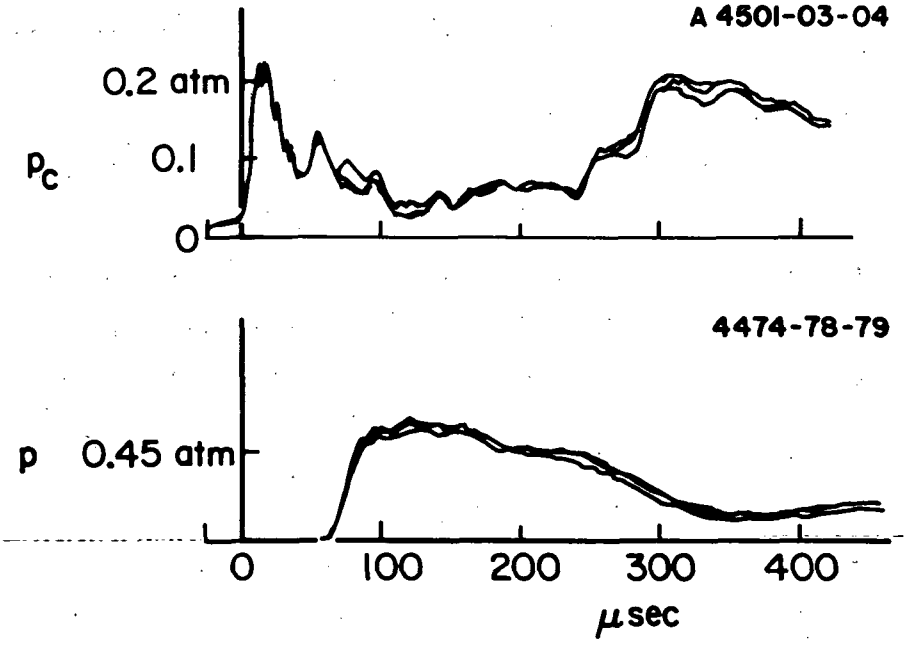

b) PRESSURE MEASUREMENTS, J = 85 kA

FIGURE II-2
AP 25-4731

The downstream pressure, on the other hand, achieves a steady value at 95 μsec and remains roughly steady at approximately 0.45 atm until 270 μsec. There is a time delay between achievement of the steady phase at the electrode insulator junction and at the downstream station due to the time of transit of the plasma between the two stations. It is important, however, to note that the duration of the steady phase is the same whether it is obtained from the terminal measurements or the pressure measurements.

Measurements of pressure and electron density indicate that the one-dimensional assumption is valid as well. Pressures were measured at a station 23 cm downstream from the electrode insulator junction, at two representative positions in the channel top, the centerline of the channel and 5 cm to one side. The values of measured pressure fall within a few per cent of each other indicating a negligible pressure gradient across the width of the channel as expected. No pressure measurements were taken across the height of the channel. However, it is reasonable to expect the pressure to remain uniform across this dimension at the downstream position, because this position is located outside the current distribution at a distance which is at least three times the characteristic distance associated with the downstream excursion of the current distribution.

A typical measurement of electron density across the height of the channel obtained spectroscopically is shown in Fig.II-3.These measurements represent an average of the electron density along the line of sight which is the width of the channel. Though the measured densities show some variation across the height of the channel, the deviations are found to be about 15 percent, so that for the purpose of the analysis electron density is treated as constant with a value equal to the average value.

For the one-dimensional assumption to be valid it is also necessary to assume one-dimensionality in the electromagnetic

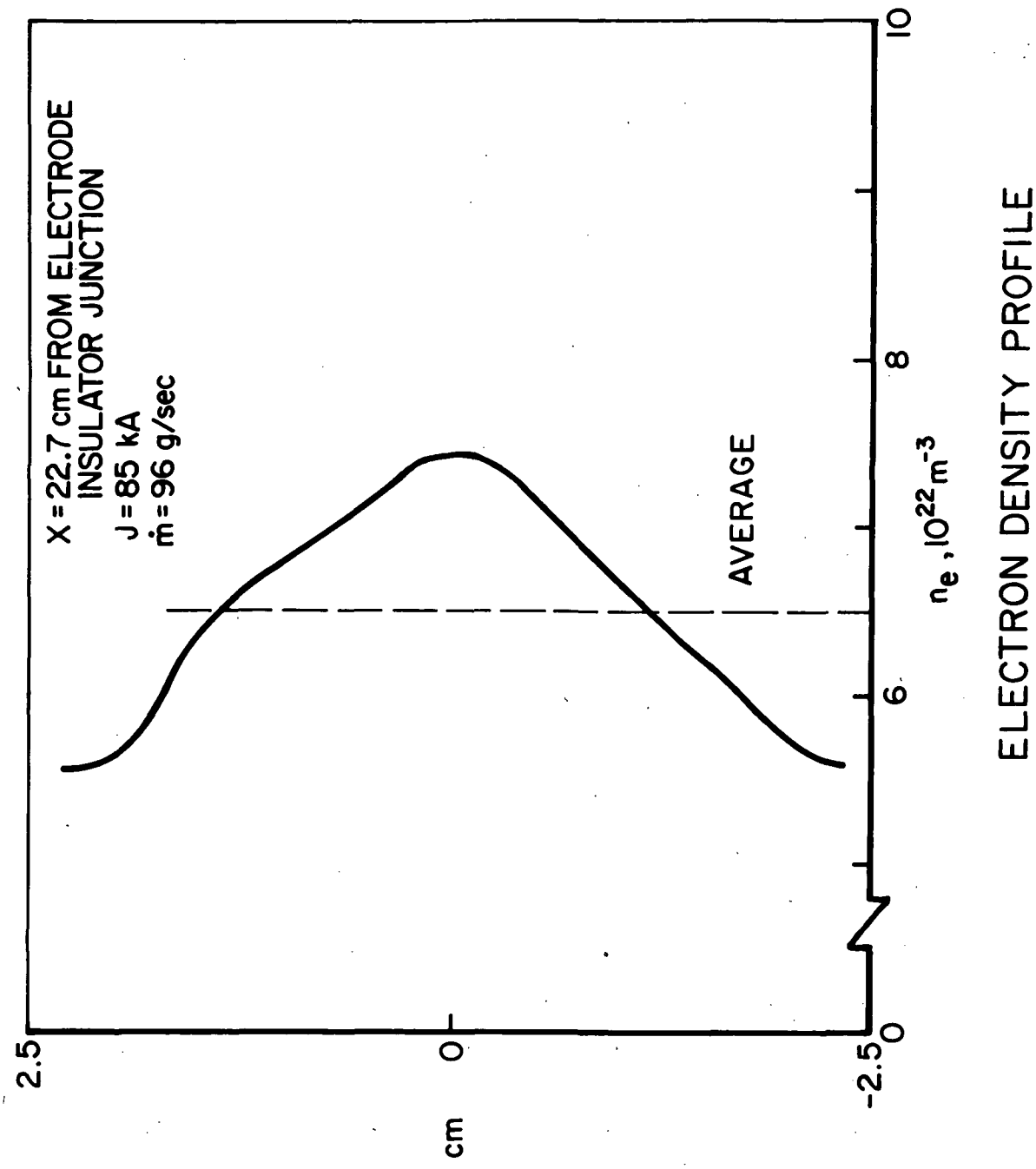

FIGURE II-3
AP 25-4732

fields as well. This assumption is based upon the small height of the channel with respect to its width and upon the uniformity of the current density in the discharge as well as in return conductors. Previous magnetic probing of the discharge in the same accelerator with similar currents [70,92] have shown that the two-dimensional effects associated with the finite size of the conductors are not too severe and that no distinct current concentrations or spokes exist. Therefore, a one-dimensional treatment of the problem is justified.

Since viscous and heat transfer effects depend quite heavily upon velocity and temperature gradients in the flow which are not known a priori as well as on transport properties of the fluid, the analysis will be carried out on the presumption that these effects are small and can be neglected. It will be later shown that this is indeed the case.

E. Interpretation of the Data

The experimental data can now be interpreted within the framework of the steady one-dimensional conservation relations stated in Sec. C. The analysis will be carried out between two stations in the channel:

Station 1. - Located 13.7 cm upstream of the electrode insulator junction at the same axial position as the injectors, and,

Station 2. - Located 22.7 cm downstream of the electrode insulator junction.

1. Momentum Conservation

The pressure p_1, density ρ_1, and velocity u_1 at a station 1 are estimated on the basis of a mass flow of 96 g/sec assuming choked flow at the orifices. Under these assumptions:

$$p_1 = 0.7 \times 10^5 \ n/m^2$$

$$\rho_1 = 0.9 \ kg/m^3$$

$$u_1 = 3.7 \times 10^2 \ m/s$$

For a current of 57 kA, which is the lowest current used,

$$\frac{\mu_0 J^2 A}{2w^2} = 7\times10^2\, n \gg 0.35\times10^2\, n = \rho_1 u_1^2 A_1$$

$$\frac{\mu_0 J^2 A}{2w^2} = 7\times10^2\, n \gg 0.2\times10^2\, n = p_1 A_1$$

$$\frac{\mu_0 J^2}{2w^2} = 9\times10^4\, n/m^2 \gg 0.5\times10^4\, n/m^2 = p_c$$

Neglecting these terms, the momentum equation becomes:

$$p + \rho u^2 = \frac{\mu_0 J^2}{2w^2} \tag{27}$$

Table I summarizes the values of the magnetic pressure at station 1, $\frac{\mu_0 J^2}{2w^2}$, the static pressure at station 2, p, and the electron density at station 2, n_e. All these quantities are determined experimentally. Under the assumption of full (single) ionization, the density of the fluid ρ becomes:

$$\rho = n_e m_i$$

where m_i is the mass of the argon ions.

There is strong experimental evidence to suggest that the full (single) ionization assumption is indeed correct. Spectroscopic observation of the flow in this accelerator and in a coaxial MPD accelerator operating with similar current densities indicate that singly ionized argon is the dominant species in the flow.(Sect.III-B) Further, there is no energy source to increase the ionization level downstream. Extensive recombination, on the other hand, is not believed to take place in the bulk of the plasma since the constant area-channel precludes expansion and cooling of the flow.

Using the measured values of p, J and n_e and the subsequently calculated density ρ, equation (27) is used to determine the average velocity u necessary to conserve momentum across the discharge. This value is compared in

TABLE I - MOMENTUM CONSERVATION

$\dot{m}$ (10^{-1}kg/sec)	J (10^{3}A)	$\mu_o J^2/2w^2$ (10^{5}n/m^2)	p (10^{5}n/m^2)	n_e (10^{22}m^{-3})	ρ (10^{-3}kg/m^3)	ρu^2 (10^{5}n/m^2)	u (10^{3}m/sec)	u_D (10^{3}m/sec)	$\dot{m}_p$ (10^{-1}kg/sec)
.96	85	2.0	.45	6.5	4.3	1.55	6.0	6.8	2.02
.96	71	1.4	.41	4.8	3.2	1.0	5.6	5.3	1.37
.96	57	.90	.31	3.5	2.3	.60	5.1	4.5	.90

TABLE II - ENERGY CONSERVATION

$\dot{m}$ (10^{-1}kg/sec)	J (10^{3}A)	V (10^{2}V)	T_i (10^{4}°K)	h (10^{7}m^2/sec^2)	$u^2/2$ (10^{7}m^2/sec^2)	$\rho uA(h+u^2/2$ (10^{7} w)	αVJ (10^{7}watts)	$\frac{uA(h+u^2/2}{\alpha VJ}$	$\frac{u^2/2}{h}$	V_{uB} V	$\frac{V_{uB}}{\alpha V - V_{uB}}$
.96	85	2.7	3.0	6.6	1.8	1.7	2.0	.85	.27	43	.23
.96	71	2.3	4.3	7.2	1.6	1.2	1.4	.85	.22	33	.20
.96	57	1.9	4.5	7.4	1.3	.67	.9	.75	.18	24	.18

the table with the velocity obtained from a Doppler shift measurement u_D. The agreement between the calculated velocity and measured velocity is good verifying the several assumptions involved in the calculation.

The column m_p shows the mass flow calculated on the basis of the measured densities and calculated velocities at station 2 for the three currents studied. It is found that the output mass flow is a strong function of current despite the fact that the input mass flow is fixed at 96g/sec. This indicates that mass is ingested from the gas dynamic flow established prior to breakdown, or from electrode and insulator ablation.

2. Energy Conservation

On the basis of the properties of the flow through the injectors it is found that the inlet kinetic energy is negligible with respect to the input electrical energy to the flow, i.e.

$$\rho_1 u_1 A_1 \left(h_1 + \frac{u_1^2}{2}\right) \ll \alpha V J$$

With this approximation, the energy equation becomes:

$$\rho u A \left(h + \frac{u^2}{2}\right) = \alpha V J \qquad (28)$$

The enthalpy in the exhaust flow could be expressed as a function of density and pressure. It is, however, more convenient to express it as a function of temperature and pressure for reasons which will become clear below.

Since there are no reliable temperature measurements in this accelerator, the temperatures will have to be estimated on the basis of an equation of state which takes into account the fact that the fluid is fully (singly) ionized. Experimentally, it has been found that in accelerators of this type, the electron temperature remains nearly constant at 1.5-2.0 eV over a wide range of operation conditions.[111] Thus, the ion temperature can be calculated from the measured

pressure and electron number density, the assumed electron temperature, and the following expression:

$$p = n_e k T_e + n_i k T_i = n_e k (T_e + T_i) \tag{29}$$

where T_e is the electron temperature and T_i is the ion temperature. Table II shows the values of ion temperature obtained with this equation assuming an electron temperature of $2 \times 10^4 {}^{o}K$.

Consistant with the two fluid model incorporated in the equation of state presented above, the enthalpy can be expressed as:

$$h = h(T_i, T_e, p) \tag{30}$$

Here, T_i describes the energy content of the random ion motion while T_e describes the energy content of the electron random motion and of the excited states which in this case include ionization.

The electron temperature never reaches the ion temperature since thermal energy transferred from ions to electrons easily passes from the electron thermal modes into the excited state system. This process can account for the constant electron temperatures observed. With this model, the expression for the enthalpy becomes:[105]

$$h = \int_{T_i}^{T_e} C_p \, dT + \frac{5}{2} R \int_{T_e}^{T_i} dT \tag{31}$$

The first term can be obtained directly from a Mollier chart for argon while the second may be evaluated directly for each calculated value of ion temperature.

Assuming an electron temperature of $2 \times 10^4 {}^{o}K$ the expression for the enthalpy becomes:

$$h = \left(5 \times 10^7 + 5.22 \times 10^2 \, T_i/{}_{o}K\right) m^2/s^2 \tag{32}$$

The column h in Table II displays the value of the enthalpy obtained with the above expression on the basis of the calculated ion temperatures. The total power in the exhaust,

$\rho uA(h + \frac{1}{2} u^2)$ can then be calculated and is also shown in the table. This power should be compared to the total power available to the flow, $\alpha V J$, defined previously. For an MPD accelerator of comparable size and range of operation, the cathode and anode falls are typically of the order of 10 and 20 volts respectively.[111,113] It is therefore estimated that between 10 and 20 percent of the input power is lost to the electrodes resulting in a value of $\alpha = 0.85$. The total input power available to the flow, 0.85 VJ, is shown in the next column and is seen to compare very favorably to the total power in the exhaust.

3. The Energy Deposition Ratio

The initial energy deposition ratio, which is the central interest of this study can be calculated using two approaches. One approach uses the ratio of streaming to thermal energy in the exhaust under the assumption that the constant area channel does not allow acceleration of the flow downstream of the discharge region. The energy deposition ratio calculated by this method is shown in Table II in the column labeled $\frac{u^2/2}{h}$. According to the calculations only about 20 percent of the energy in the exhaust appears as directed kinetic energy.

The other approach uses the ratio of the motional emf and resistive components of the terminal voltage across the accelerator. To define the motional emf, the energy equation is used in the form:

$$W = \int_V \vec{E} \cdot \vec{j} \, dV \tag{33}$$

where W is the rate of energy input to the plasma by the external electric field and $\vec{j}$ is the current density. In the plasma frame of reference, the electric field is

$$\vec{E}' = \vec{E} + \vec{u} \times \vec{B} \tag{34}$$

where $\vec{B}$ is the local magnetic field and $\vec{u}$ is the velocity of the plasma. Substituting the equation above in the energy equation, the total energy input to the plasma by the external

fields becomes:

$$W = \int_V \vec{E}' \cdot \vec{j}\, dV - \int_V (\vec{u} \times \vec{B}) \cdot \vec{j}\, dV \qquad (35)$$

Since the total energy deposited in the streaming plasma can be written as αVJ where as before α is the fraction of the input power available to the flow, the voltage drop minus the fall voltages can be written as the sum of two voltages:

$$\alpha V = \frac{1}{J} \int_V \vec{E}' \cdot \vec{j}\, dV - \frac{1}{J} \int_V (\vec{u} \times \vec{B}) \cdot \vec{j}\, dV$$

$$= V_R + V_{uB}$$

where V_R is defined as the resistive voltage drop across the accelerator while V_{uB} is the motional emf.

To perform a rigorous calculation of V_{uB} a detailed knowledge of the velocity and current density in the acceleration region is required. Its magnitude, however, can be estimated by assuming reasonable profiles for the velocity u, current density j, and magnetic field B. Table III summarizes the results of calculations made for different arbitrary profiles. In this table, B_1 is the magnetic field upstream of the current distribution, u is the downstream velocity, w is the width of the accelerator, δ is the width of the current distribution and J is the total current. The table shows that the motional emf takes the form:

$$V_{uB} = u B_1 h Q \qquad (36)$$

where Q is a factor which depends on the particular profiles chosen and has a value that ranges between 0.16 and 0.41 for the profiles shown.

The ratio of motional emf to resistive drop is shown in the column $V_{uB}/\alpha V - V_{uB}$. The value of V_{uB} is calculated assuming that there is no downstream expansion of the flow. Therefore, the measured velocities accurately reflect the

TABLE III - V_{uB} FOR DIFFERENT VELOCITY AND CURRENT DENSITY DISTRIBUTIONS
for: $0 \leq x \leq \delta$

	u	B	j	V_{uB}
I	$\frac{ux}{\delta}$	$B_1\left(1 - \frac{x}{\delta}\right)$	$\frac{J}{w\delta}$	$\frac{1}{6}\ uhB_1$
II	$2u\left(\frac{x}{\delta} - \frac{x^2}{2\delta^2}\right)$	$B_1\left(1 - \frac{x}{\delta}\right)$	$\frac{J}{w\delta}$	$\frac{1}{4}\ uhB_1$
III	$u \sin \frac{\pi x}{2\delta}$	$B_1 \cos \frac{\pi x}{2\delta}$	$\frac{\pi}{2\delta}\ \frac{J}{w} \sin \frac{\pi x}{2\delta}$	$\frac{1}{3}\ uhB_1$
IV	$\frac{ux}{\delta}$	$B_F \cos \frac{\pi x}{2\delta}$	$\frac{\pi}{2\delta}\ \frac{J}{w} \sin \frac{\pi x}{2\delta}$	$\frac{1}{4}\ uhB_1$
V	$u \sin \frac{\pi x}{2\delta}$	$B_1\left(1 - \frac{x}{\delta}\right)$	$\frac{J}{w\delta}$	$\frac{4}{\pi^2}\ uhB_1$

velocity of the fluid at the exit of the current distribution. The geometric factor Q for this calculation is set at 0.20.

There is reasonable agreement between the energy deposition ratio based on kinetic energy and enthalpy and the ratio based on motional emf and resistive voltage drops. Both these ratios point to the conclusion that the discharge itself imparts less energy to the flow by direct body acceleration than by resistive heating. In the absence of downstream expansion this predicates low exhaust speeds and high downstream pressures and temperatures. Conversely, it seems reasonable to infer that the comparatively high exhaust speeds found in conventional MPD arcs of the same power must be derived in substantial part from electrothermal conversion from the high enthalpy arc plasma via the downstream expansion permitted in this geometry.

F. Appendix: Viscous Dissipation and Heat Transfer

The calculations performed in the previous section are based on the assumptions that viscous drag and heat transfer to the walls are not severe. The values of the flow properties previously calculated and approximate values of the transport properties published in the literature can be used to estimate the magnitude of these effects.

The Reynolds number of the flow based upon the length of the channel is, for the 85kA current pulse:

$$Re_\ell = \frac{\rho u \ell}{\mu} = 3 \times 10^5$$

where [II-3] $\ell = 2 \times 10^{-1}$ m and $\mu = 2 \times 10^{-5}$ kg/m-s

For an incompressible turbulent boundary layer, the friction coefficient is: [II-4]

$$f = \frac{0.03}{(Re_\ell)^{1/5}} = 2.4 \times 10^{-3}$$

The ratio of viscous forces to electromagnetic forces becomes:

$$\frac{F_v}{F_M} = \frac{f \rho u^2 2\ell w \left(\frac{h}{w} + 1\right)}{h w (\mu_0 J^2/2w^2)} = 2 \times 10^{-2}$$

where $h = 5 \times 10^{-2}$ m and $w = 1.5 \times 10^{-2}$ m. It is therefore justified to drop the viscous dissipation from the momentum and energy equations.

It is not possible to perform a similar calculation for the heat transfer to the channel walls due to the complex nature of the working fluid. However, it is possible to estimate the magnitude of the heat transfer from the ratio of the power delivered to the flow to the total power in the exhaust which is shown in the column $\frac{\rho u A (h + u^2/2)}{\alpha V J}$ in Table II. According to this ratio, 75 to 85% of the power delivered to the beam appears as power in the exhaust. On this basis, it is estimated that 15 to 25% of the input power is lost by either heat transfer to the channel walls or by radiation.

III. QUASI-STEADY DISCHARGE PROPERTIES

A. Time-Resolved Interferometry of the MPD Exhaust Plume (Bruckner)

An extensive time-resolved interferometric survey of the exhaust plume of the MPD arc has been carried out to map the axial and radial profiles of the velocity and temperature of argon II, which is the spectroscopically dominant state of the propellant in the discharge. Detailed analysis of the data illuminates various aspects of the discharge, such as the relative roles of electromagnetic and electrothermal acceleration mechanisms, and the partition of directed kinetic and random thermal energies in the exhaust flow. A full treatment of the subject will appear in a forthcoming Ph.D. dissertation.[125]

Exhaust velocities have been measured in the past by means of displaced pairs of biased double electrostatic probes which detect the time of flight of local fluctuations in the plasma number density.[85,97,118] Unfortunately such probes suffer from the fact that their presence in the exhaust jet disturbs the flow and they are unable to distinguish particle motion from wave motion. An independent measurement of the exhaust velocity can be made by observation of the Doppler shift of selected spectral lines. Although such a spectroscopic technique does not disturb the plasma flow, it is not capable of direct local measurements. Rather, the observed line shift is the integrated effect of all emitters along the line of sight and thus is distorted by radial and axial distributions of emitter number density, temperature, and velocity. In principle, the complete velocity and temperature distribution of the jet can be obtained by properly unfolding detailed spectroscopic observations at selected angles to the axis of the discharge[III-1] as long as the jet is cylindrically symmetric.

In order to achieve the high spectral resolution necessary to detect velocities of the order of 10^4 m/sec, we have used a Fabry-Perot interferometer which can be scanned

electrically, via a piezoelectric mount on one of the interferometer plates, at selected times during the arc pulse. A schematic of the interferometer and its supporting optics is shown in Fig.III-1. The output of the pulsed argon ion laser is superimposed on the optical train to provide a convenient sharp reference wavelength. The pinhole behind the projection lens, L_4, selects the center of the scanning fringe pattern produced by the Fabry-Perot, and acts as a spatial filter defining, in conjunction with the lenses ahead of it, the conical volume of plasma which will contribute light to the photomultiplier detector. The mirror M_1, can be adjusted by means of two micrometer screws to select for examination any desired line of sight through the exhaust plume. The entire system is enclosed in a sound absorbing box and mounted on a heavy table which is vibration-isolated from the floor.

The 4880 Å line of argon II has been chosen for study because it is in a relatively clean region of the arc spectrum where there exist only a few relatively faint impurity lines[119], and because it is readily available from the laser as the unshifted wavelength standard.

Complete radial surveys have been done at three lines of sight which intersect the discharge axis at distances of 9.1 cm, 15.8 cm, and 39.8 cm from the anode face, at angles of 38.9°, 40.6°, and 36.3° respectively. Up to 26 radial positions for each axial station were examined, the MPD arc being fired three to eight times at each to acquire enough data to smooth out random shot-to-shot variations. Fig.III-2 displays a typical data record for the 16.8 kA, 5.9 g/sec arc condition, at the 9.1 cm axial position, on axis. The spectral line is scanned several times in succession during the discharge, the observed fringe separation, or free spectral range, being 0.74 Å in this case. The observed Doppler shift corresponds to an axial component of velocity of nearly 10^4 m/sec. Components of velocity as high as 2.0×10^4 m/sec have been detected at the 39.8 cm location. The radial distribution of axial velocities appears to be relatively

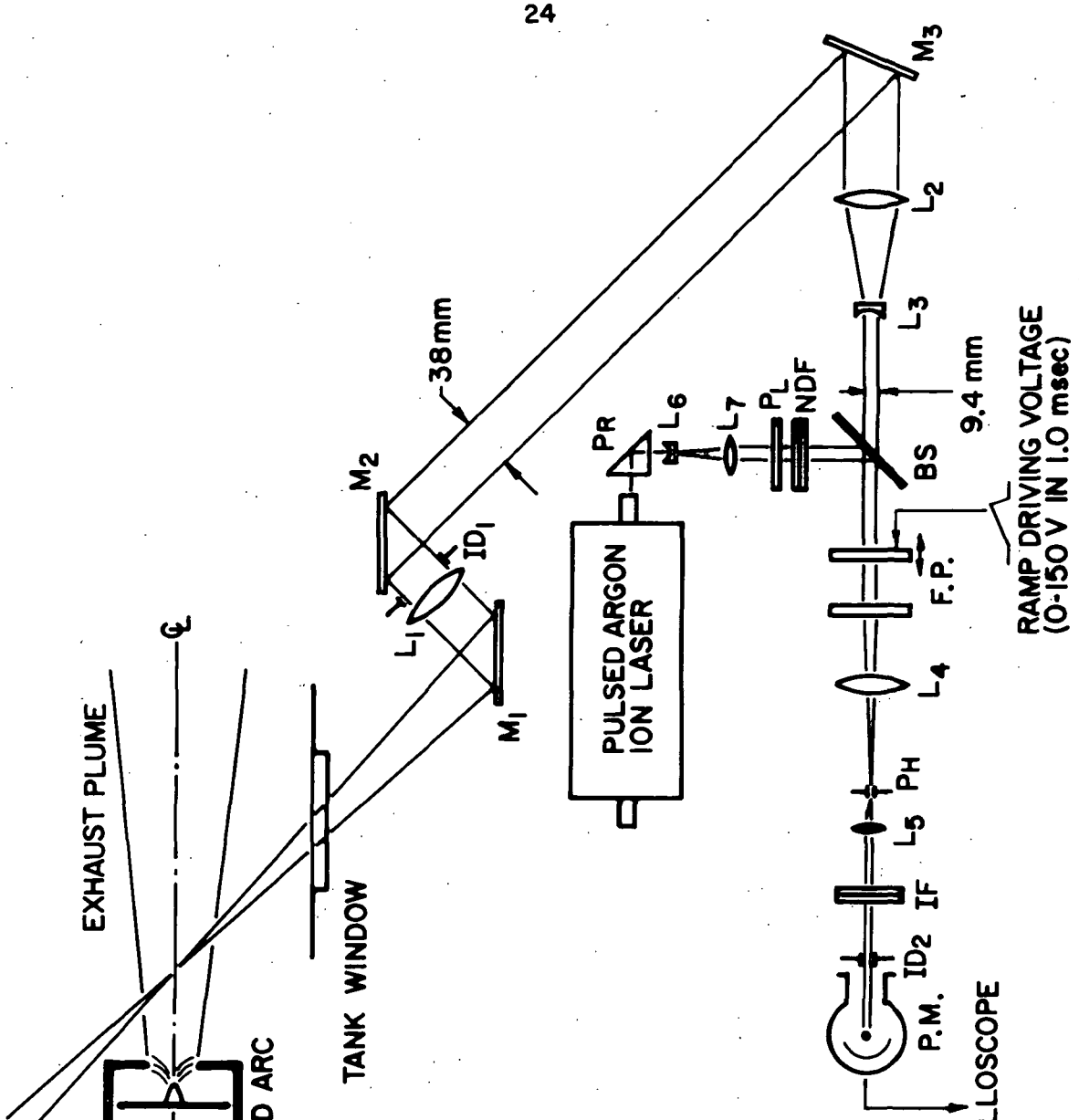

LEGEND

M_1	Traversing Mirror (Micrometer Adjusted)
M_2, M_3	Adjustable Mirrors
L_1	Objective Lens (127 cm F.L.)
L_2	Beam Reducing Lenses
L_3	Fringe Projection Lens
L_4	Collimating Lens
L_5	Laser Beam Expanding Lenses
L_6	Clear Glass Beam Splitter
L_7	Fabry-Perot Interferometer
BS	Pinhole (0.08 cm Dia.)
F.P.	Polarizer
P_H	Right Angle Prism
P_L	Neutral Density Filters
P_R	Interference Filter 4880 Å (10 Å B.W.)
NDF	Iris Diaphragms
IF	Photomultiplier Tube (RCA 1P28)
ID_1	
ID_2	
P.M.	

FIGURE III-1
AP25-4738

SET-UP FOR TIME-RESOLVED INTERFEROMETRY

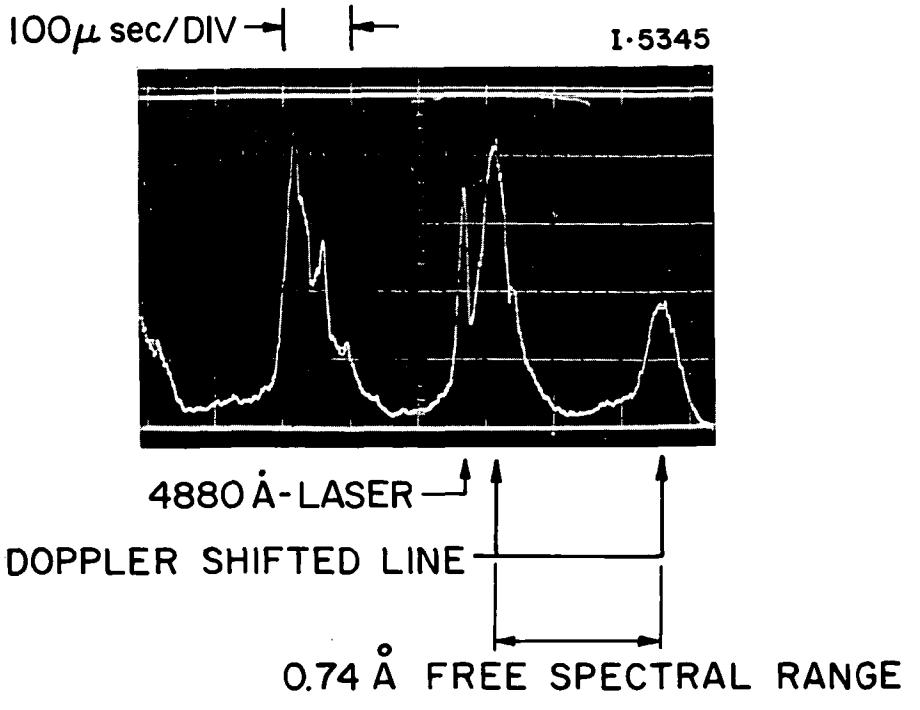

DOPPLER SHIFTED ARGON II LINE PROFILE

FIGURE III-2
AP 25·P-378

flat, however, a detailed map must await reduction of the transverse radiance and temperature profiles.

An interesting effect observed in the velocity survey is the radial distribution of line radiance, which shows a curious dip and a second peak off-axis, Fig. III-3. This suggests a more complicated jet structure than has heretofore been assumed.

Following the velocity measurements, the optics were rearranged to carry out radial temperature surveys perpendicular to the discharge axis at four axial distances downstream of the anode face: 4.6 cm, 10.9 cm, 15.9 cm, and 30.6 cm. It was during these experiments that a prominent splitting of the spectral line was discovered. This is well displayed in Fig. III-4, which was obtained at 10.9 cm from the anode, on axis. This effect is caused by a Doppler shift resulting from substantial radial components of velocity in the exhaust plume. This radial velocity is seen at all four axial stations, increasing in the downstream direction, as shown in Fig. III-5a and reaching a maximum of about 5400 m/sec. The very sharp separation of the approaching and receding Doppler components of the spectral line indicates that the emitting ions are concentrated in two distinct regions of the jet across its diameter. This model is supported qualitatively by the radial radiance profiles seen in the velocity survey and also in the survey perpendicular to the discharge axis. A fortuitous result of this structure is that the strong splitting of the spectral line allows relatively unambiguous temperature measurement of the exhaust jet. From the Doppler width of the individual line components, the temperature of the argon II was calculated and plotted in Fig. III-5b, as a function of axial distance. It is seen that the ion temperature drops quickly to a value less than 1 eV, which reflects efficient conversion of random thermal energy to directed kinetic energy of the jet.

As an additional check on exhaust velocity, the optics were aimed down the Plexiglas tank to observe the discharge

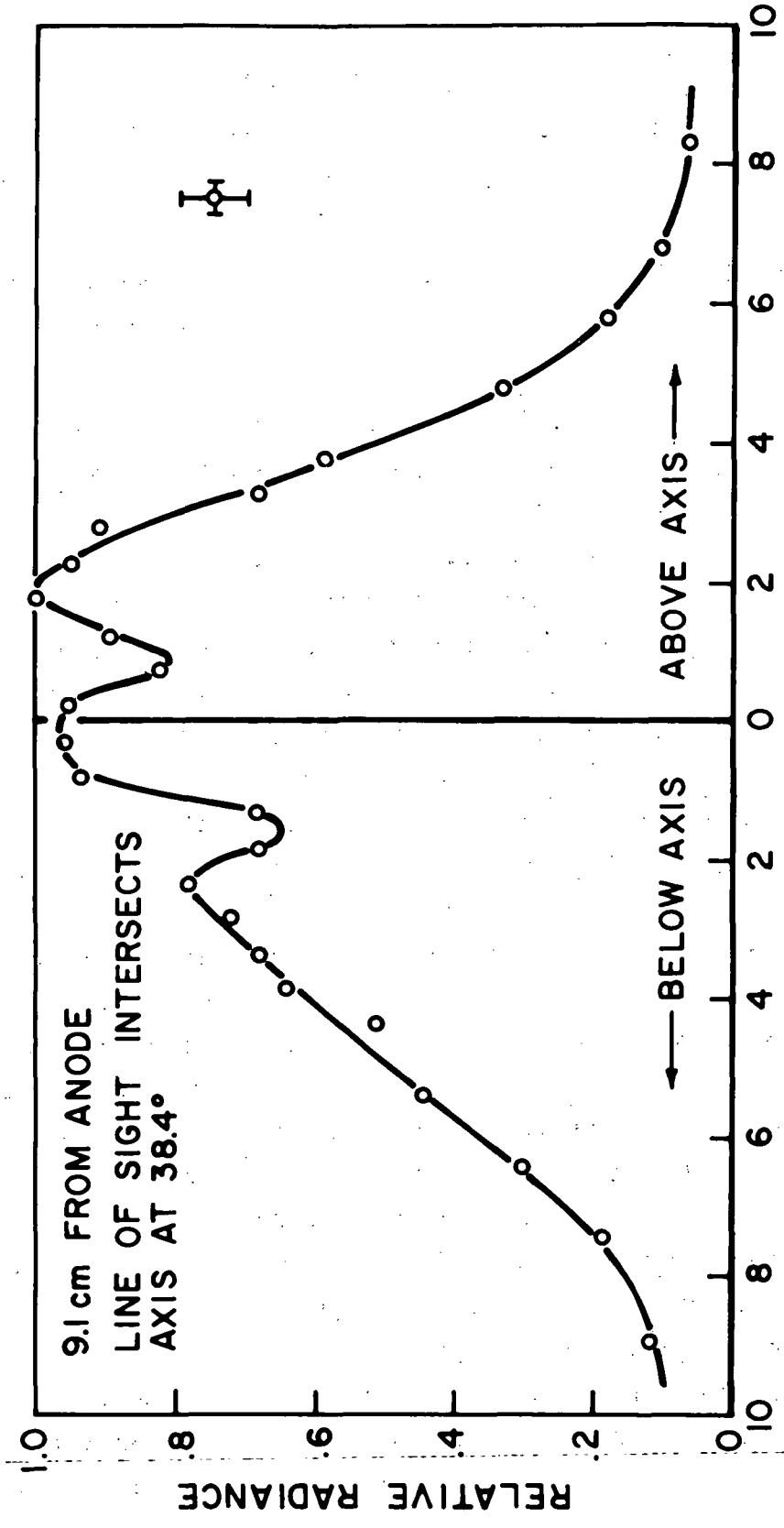

FIGURE III-3
AP25-4733

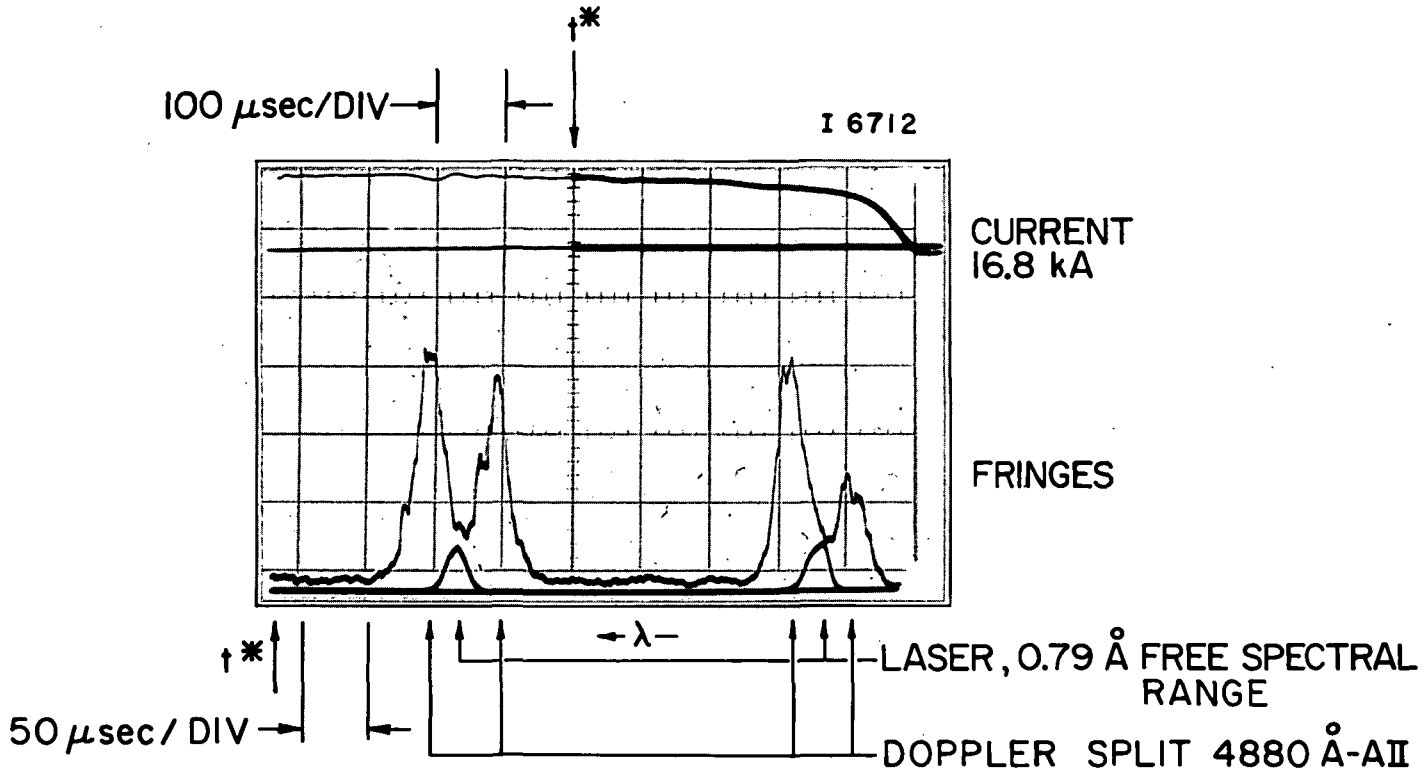

THE 4880 SPECTRAL LINE OF ARGON II TAKEN
PERPENDICULAR TO DISCHARGE AXIS
10.9 cm FROM ANODE

FIGURE III-4
AP 25·P 395

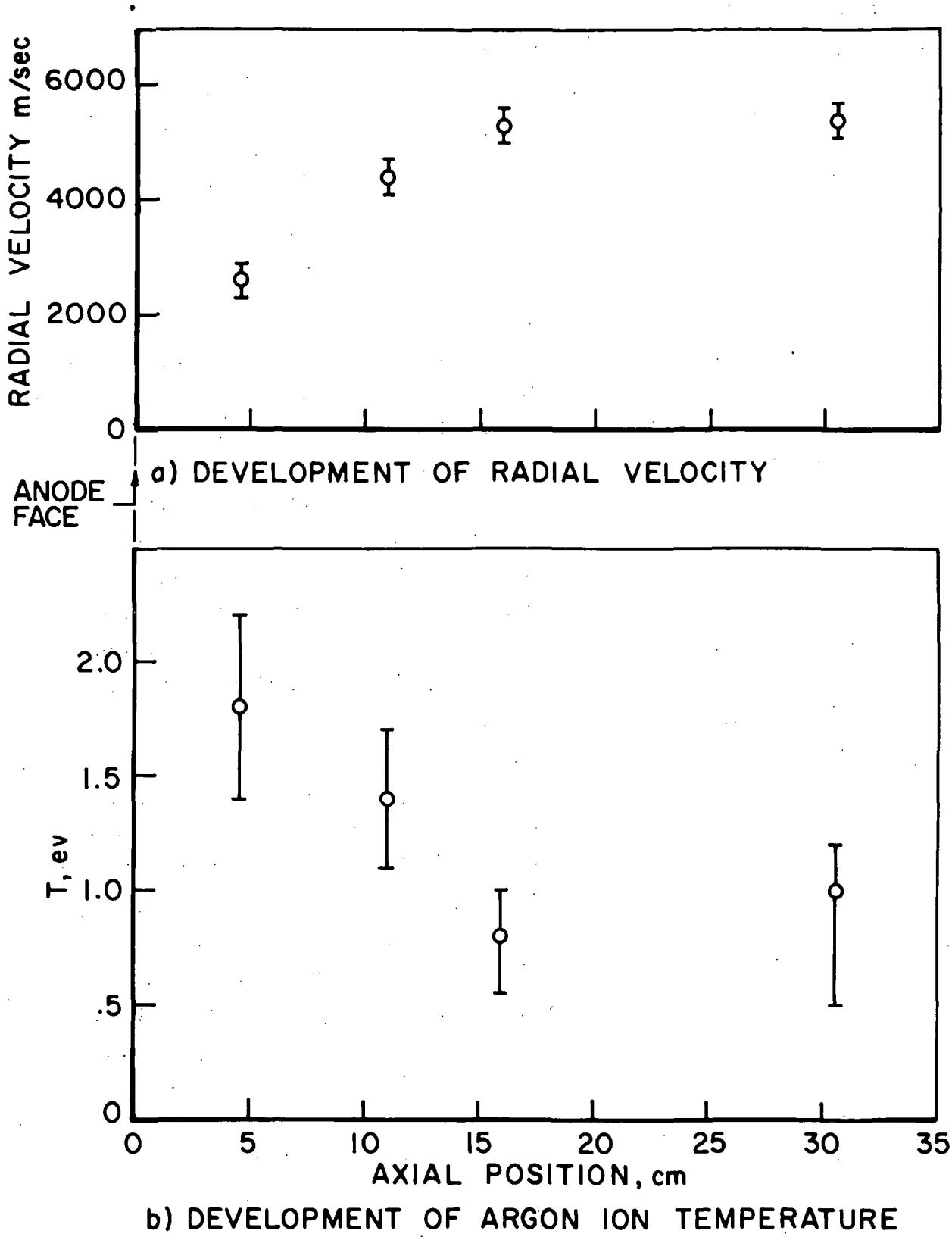

FIGURE III-5
AP25-4734

axially, i.e., head-on. The exhaust plume was examined at various radii and at several circumferential angles. It was found that the plume exhibits a complex, lobed structure, with the argon II seemingly concentrated in six well-defined jets which are angularly in line with the six propellant injector ports in the discharge chamber. This result correlates well with the previous remarks on jet structure. The particle velocities in these jets range from about 5×10^3 m/sec at the anode orifice to about 1.2×10^4 m/sec approximately 20 cm downstream.

In order to verify the existence of the complex six-jet structure of the exhaust plume, the discharge was photographed through the 4880 Å interference filter to reveal the spatial distribution of the argon II emitters. The results, shown in Figs. III-6a and III-6b emphatically exhibit this interesting structure. The six argon II jets (three of which are seen in the side view) line up directly with the injector ports, suggesting that the injected gas streams remain well-collimated through the discharge. Because this structure had not been detected in the past, and because spectrograms reveal an abundance of carbon and other impurities in the jet,[105] it was hypothesized that the regions between the argon jets are filled with ablation products from the Plexiglas rear wall of the discharge chamber. This is confirmed by Figs. III-7a and III-7b which show photographs of the discharge taken without the 4880 Å line filter, thus making all wavelengths visible. In the side view the jet structure has smeared out and is only faintly visible. In the end view (Fig. III-7b) it can be seen that the dark spaces between the bright argon jets visible in Fig. III-6b are now themselves luminous and extend radially outward between the injectors to the chamber walls, in a starlike pattern. This remarkable argon II jet structure had never before been detected since the various diagnostic tools used in the past, such as magnetic probes, electrostatic probes, pressure probes, etc. are unable to distinguish among the various ionic and atomic species present in the discharge.

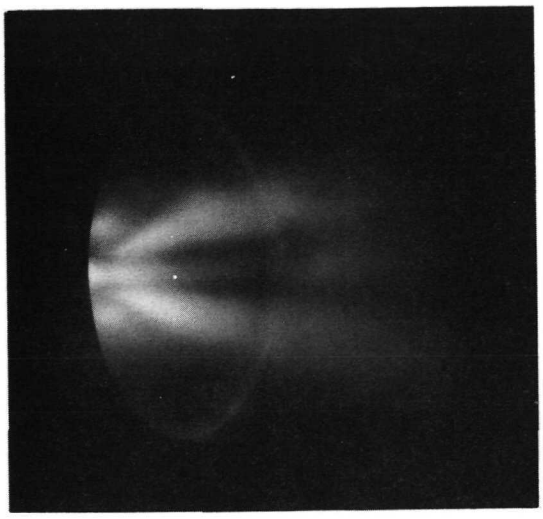

a) SIDE VIEW OF DISCHARGE AT 4880 Å

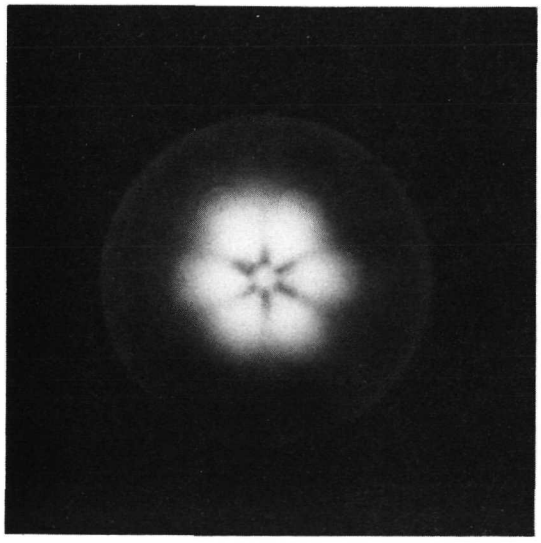

b) HEAD-ON VIEW OF DISCHARGE AT 4880 Å

FIGURE III-6
AP25·P396

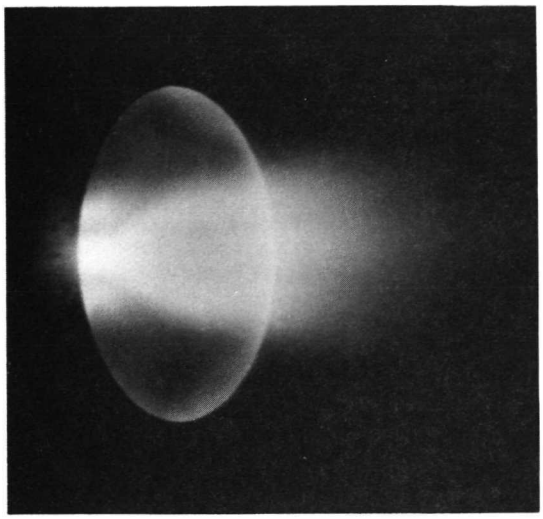

a) SIDE VIEW OF DISCHARGE AT ALL WAVELENGTHS

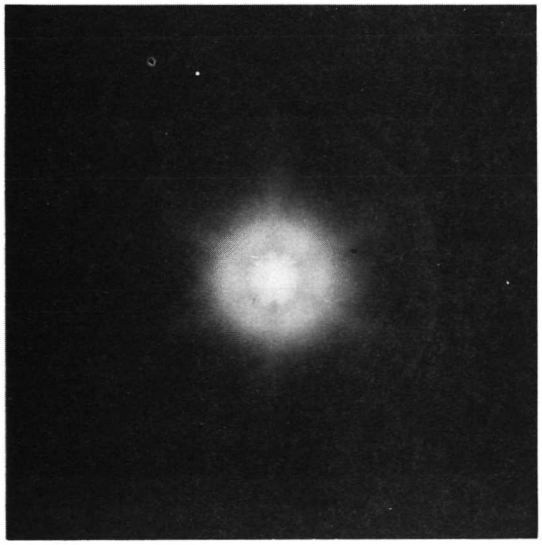

b) HEAD-ON VIEW OF DISCHARGE AT ALL WAVELENGTHS

FIGURE III-7
AP 25·P 397

With the discovery of this new phenomenon the reduction of the integrated velocity profiles to local values must be considerably modified. The results of this analysis, together with the complete temperature and intensity profiles, are discussed at length in Ref. 125.

B. Spectroscopic Studies (Hixon, von Jaskowsky)

Continuing the previous spectroscopic studies of composition, temperature, electron density and velocity in the quasi-steady MPD arc discharge,[105,109,119] additional experimental results can now be presented which establish the presence of AIII, indicate the absence of AI, and identify two distinct radial velocity components in the expansion of the exhaust flow. These data rely on earlier Kerr-cell photographs and time-resolved signals from photoelectric detectors[119,125] which show the constant level of electromagnetic radiation from the discharge, thereby allowing time-integrated photographic recording of spectra and relieving the use of complex apparatus for very short exposures.

a) Doubly ionized argon, AIII

Argon III produces several strong lines in the near ultraviolet between 3200 and 3500 Å. Because these wavelengths are near the absorption limits of the Plexiglas vacuum tank, a 7.5-cm diameter quartz window was installed in one of the tank ports. Fig. III-8 shows the complete arrangement of vacuum tank, quartz lens, and Hilger E-1 Quartz Spectrograph where the data were recorded using Royal X Pan Sheet Film. The spectrograph, focused and calibrated with a mercury 8W germicidal lamp, provided a linear dispersion between 6.4 and 8.2 Å/mm over the region of interest. A typical spectrogram, covering an 8-cm high cross section of the exhaust flow centered on the axis and 4 cm downstream of the anode, is shown in Fig. III-9. The spectra were compared to previous records of pinch discharges to identify AII reference lines of known wavelengths. The positions of intermediate lines were measured with a comparator and the corresponding wavelengths were calculated by linear interpolation.

The observed AIII lines for various current levels and mass flows of argon are listed in Table IV. For the highest current level (approximately 40 kA), at least two lines from each of

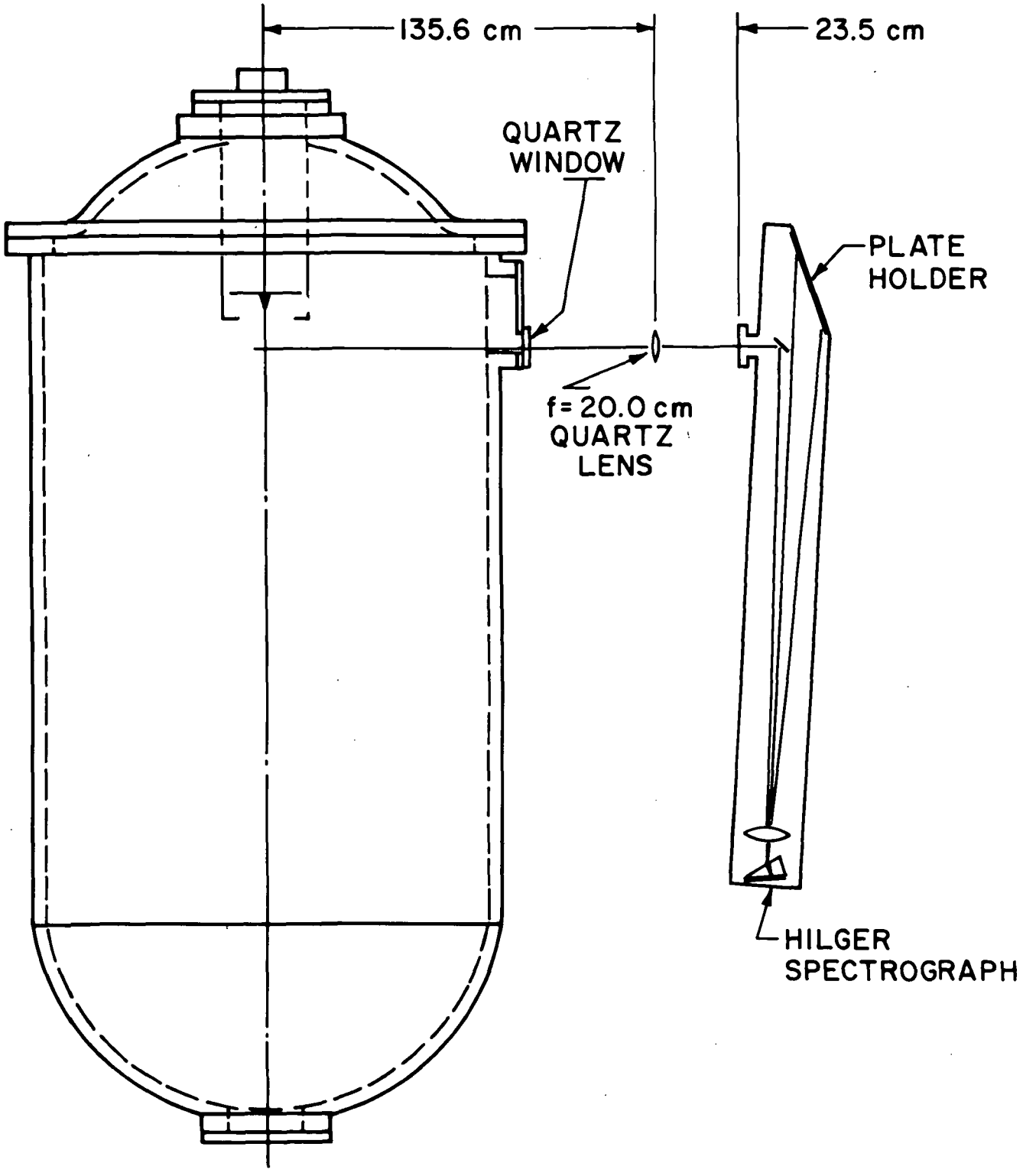

ARRANGEMENT FOR NEAR U.V. SPECTROSCOPY

FIGURE III-8
AP 25-4736

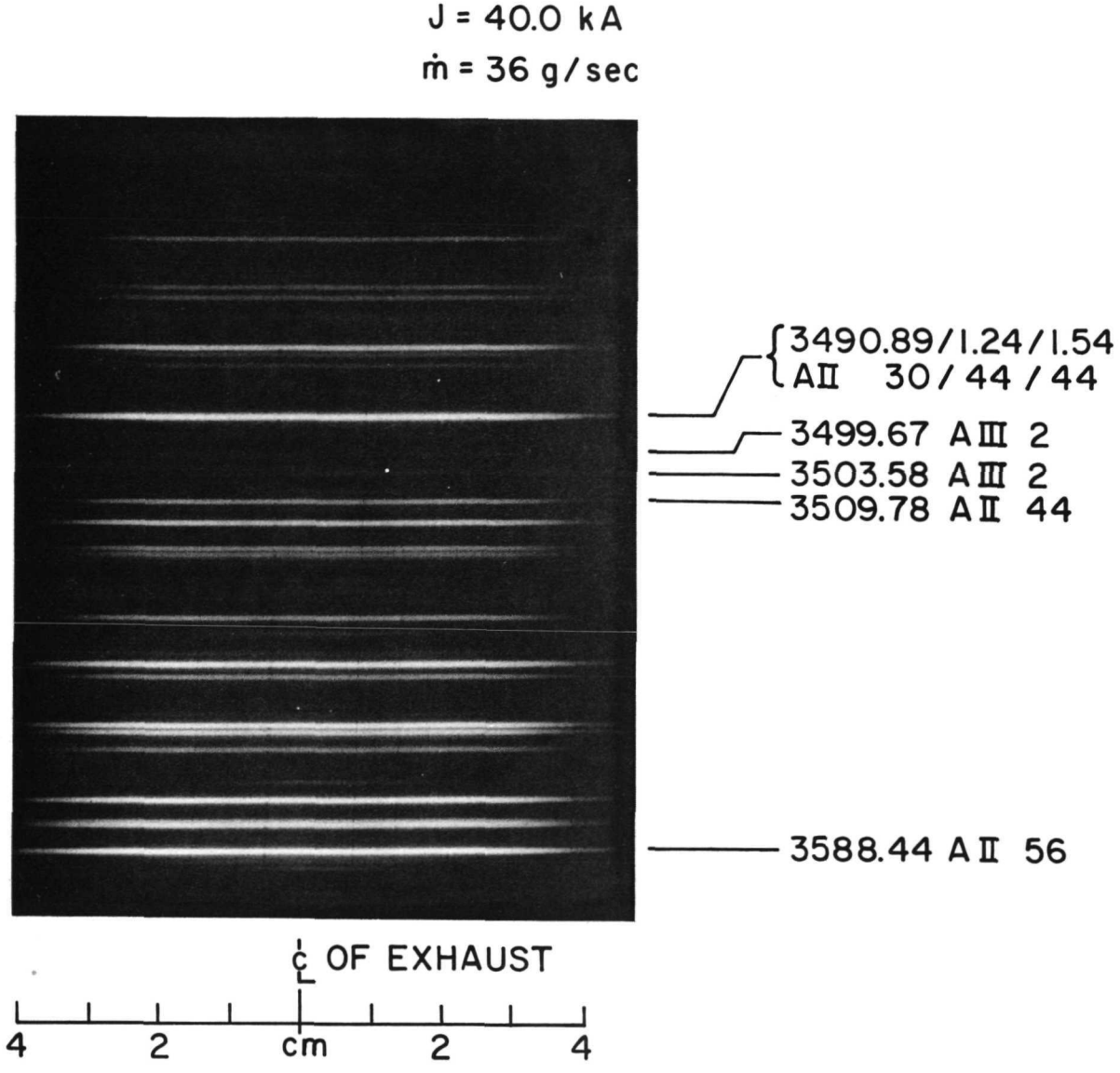

SPECTROGRAM WITH AIII LINES

FIGURE III-9
AP25·P398

TABLE IV - Observed AIII Lines

Multiplet No.	Measured λ(Å)	Identified line (Å)
J = 40 kA $\dot{m}$ = 36 g/sec		
2	3503.94	3503.58
2	3499.67	3499.64
3	3346.35	3344.72
3	3336.61	3336.13
1	3313.64	3311.25
1	3301.89	3301.88
1	3285.88	3285.85
J = 39 kA $\dot{m}$ = 6 g/sec		
3	3346.49	3344.72
3	3336.64	3336.13
1	3301.89	3301.88
1	3285.88	3285.85
J = 16 kA $\dot{m}$ = 6 g/sec		
3	3358.59	3358.49
3	3343.24	3344.72
1	3313.72	3311.25
J = 12.3 kA $\dot{m}$ = 3.8 g/sec		
No AIII		
J = 8.7 kA $\dot{m}$ = 6 g/sec		
No AIII		

the three AIII multiplets appear quite distinctly on the spectrogram. For example, two lines of multiplet No. 2 can been seen in Fig. III-9 for the 40 kA, 36 g/sec operating condition. At the 16 kA level, most of the AIII lines have faded although three lines are still faintly visible. At lower currents, for example 8.7 kA, no AIII lines are recorded and many of the less prominent AII lines have also faded out. Although the AIII intensity obviously decreases with current, the total radiation from the discharge also decreases making it difficult to determine any change in the ratio of AIII to AII over the test conditions. Nevertheless, it is clear that AII is always dominant for all data recorded. The influence of mass flow on the appearance of AIII is apparently secondary compared to this overall change in radiance with current.

Fig. III-10 shows the radial extent of the observed AII and AIII lines for the 16 kA x 6 g/sec discharge superimposed on electron density contours derived from an earlier study of the Stark widths of the H_α and H_β lines.[105] At radii beyond 4 cm, appreciable vignetting occurs, and statements about the occurrence of AII or AIII at larger radii are at best rough estimates. It is nevertheless quite evident that the AIII lines fade out about 1.5 cm from the axis while AII fades toward the edge of the field of view at a radius of about 4 cm.

b) Neutral argon, AI

Spectrograms of the MPD exhaust beam recorded previously with a glass 3-prism Steinheil spectrograph were examined for evidence of AI lines 1 cm downstream of the anode. Over 2000 Å in the visible portion of these spectrograms, the position of all lines in the vicinity of known AI spectral locations were measured with a comparator to an accuracy of a few tenths of 1 Å. Using this technique, the absence of prominent AI lines for at least six different spectral locations has been established for the 16 kA, 6 g/sec argon dis-

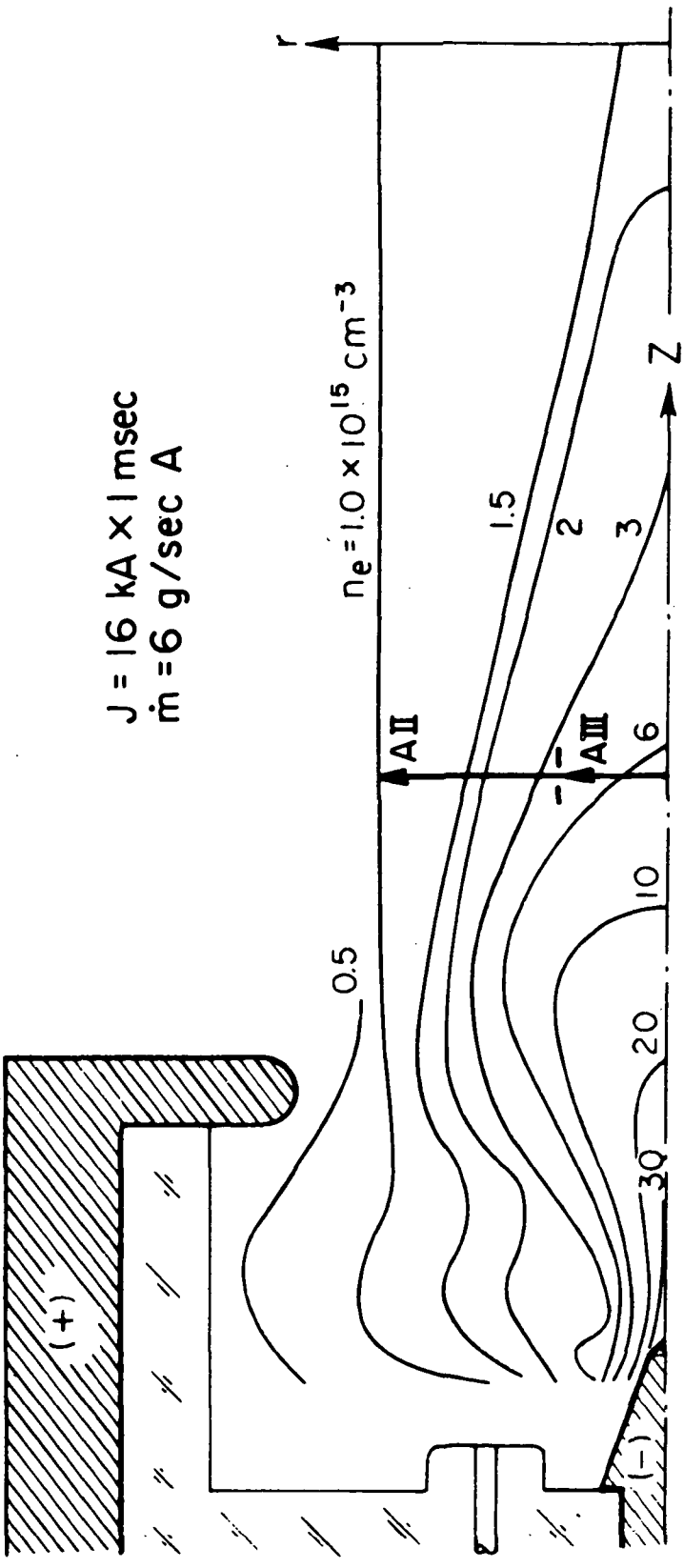

SPECTRAL LINES OF AII & AIII

FIGURE III-10
AP25-4737

charge. Considering that neutral argon must exist at the beginning and end of the current pulse, the absence of any AI evidence further strengthens the experimental observation that AII is the dominant radiating state of the propellant.

c) Radial expansion of the MPD exhaust

A continuing program to determine the heavy particle temperature in the exhaust flow by high resolution spectroscopy has revealed an interesting complication. For this study a Fabry-Perot interferometer was used in tandem with the Steinheil glass spectrograph to examine a perpendicular cross section of the exhaust flow 10 cm from the anode. Figure III-11 shows a typical interferogram of the resulting AII lines. Many of the recorded fringes near the centerline of the exhaust flow, for example the circled fringe of the 4806 Å line, consist of two clearly separated fringes due to radial velocity components, one towards and the other away from the spectrograph. The recorded Doppler shift corresponds to a radial velocity of approximately 3500 m/sec, in good agreement with that radial velocity calculated from the piezoelectrically scanned Fabry-Perot, Doppler shift measurements (see Section III-A). Consequently, the reduction of heavy particle temperatures from the Doppler width, as recorded by the Fabry-Perot-Steinheil combination, must proceed in conjunction with the reduction of the velocity profile. A survey with a decreased free spectral range for even further separation of the Doppler components is now in progress.

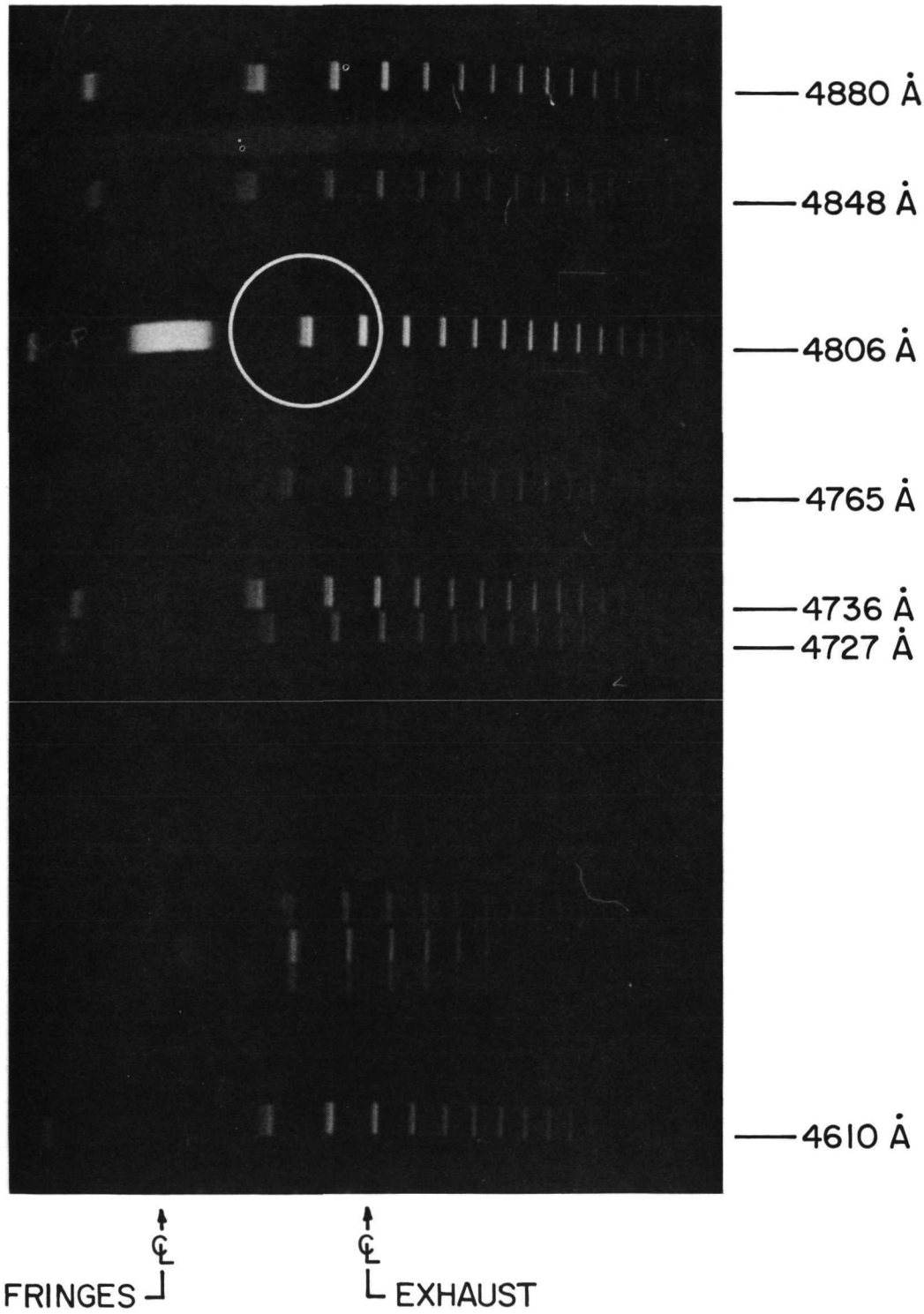

INTERFEROGRAM OF EXHAUST FLOW
10 cm FROM ANODE

FIGURE III-11
AP25 • P-379

C. Momentum Balance across the MPD Discharge (Cory)

Measurements of the impact pressure in the accelerator exhaust jet, and static pressure in the arc chamber have been performed as part of a program to investigate the conservation relations across the acceleration zone of MPD arcs. The pressure probe used for these measurements consists of a 5-cm long dielectric stub which transmits pressure, but not heat, electrical charge or induced EMF to a thoroughly shielded PZT-5 piezoelectric crystal, and a 90-cm long by 1-cm diameter backing rod whose function is to prevent reflected acoustic noise by containing the propagating pressure wave. This probe has a rise time of 10 μsec and gives distortion-free pressure records for approximately 1 msec.

The probe was first installed on the moveable platform in the Plexiglas tank to measure the momentum flux in the MPD exhaust. A radial profile of the impact pressure 28 cm from the anode for the 16 kA, 5.9 g/sec discharge is shown in Fig. III-12. The profile is nearly gaussian and decays with the square of the axial distance from the anode. Similar measurements for 1.9, 3.8, 23 and 36 g/sec argon over a range of currents from 8 to 47 kA showed this shape to be nearly invariant with mass flow and current. These features are typical of jet flow into a vacuum and suggest a model for the MPD exhaust once it has passed out of the acceleration region.

The same probe was then used to measure the pressure in the arc chamber by inserting it in a suitable static pressure tap in the chamber side wall. Measurements were obtained over the same nominal mass flow and arc current range listed above. This measured chamber pressure was then used to calculate the electrothermal thrust component. An empirical relation embracing 95% of the data is

$$\text{Electrothermal Thrust} = (2.45 \pm 0.4) \times 10^{-5} \, J^{1.5} \, \dot{m}^{0.3}$$

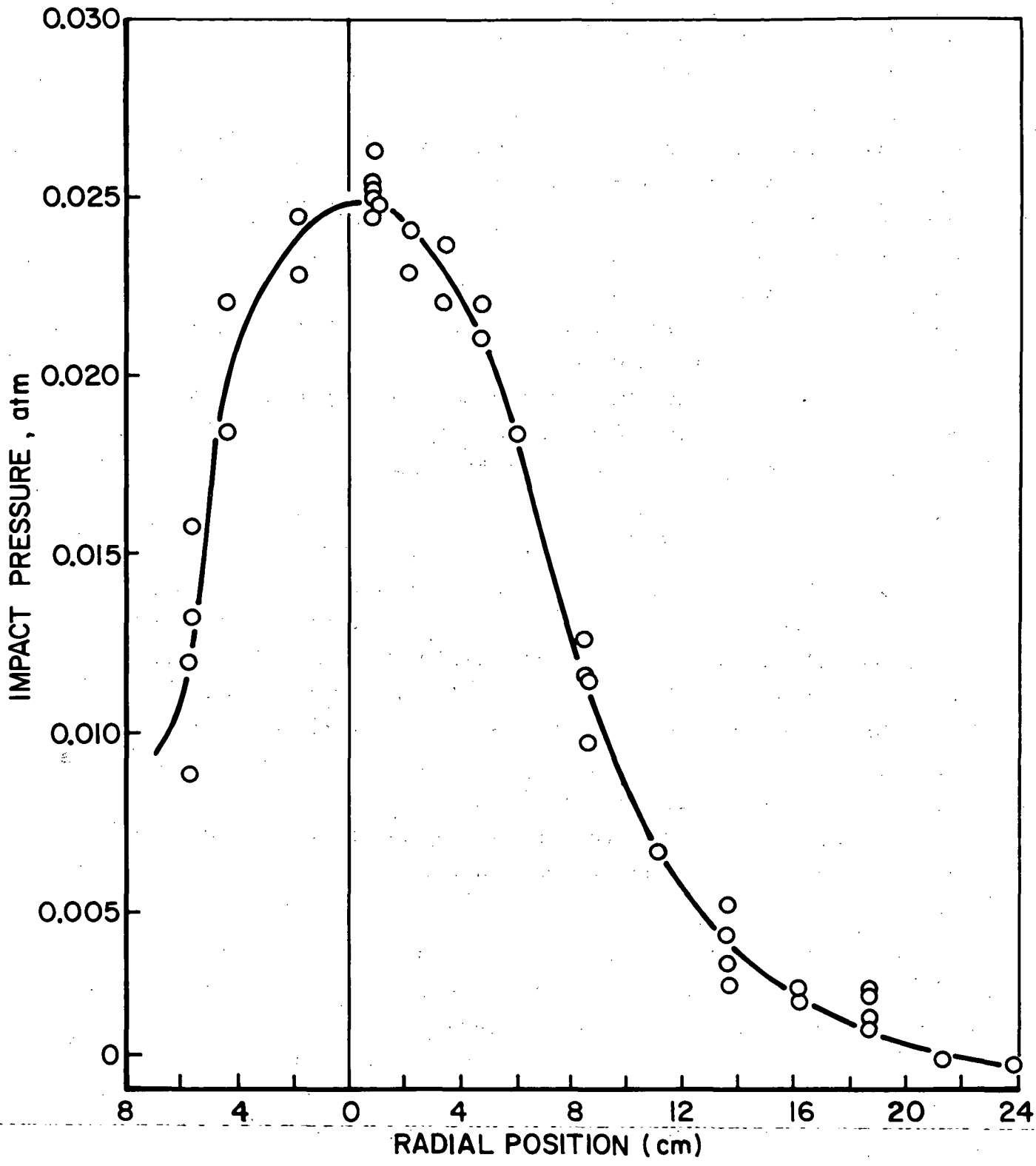

PROFILE OF IMPACT PRESSURE

FIGURE III-12
AP 25·4711

The total momentum flux from the accelerator consists of both an electromagnetic term and an electrothermal term. For our geometry and the 16 kA, 5.9 g/sec discharge, the former is evaluated from the familiar self-field expression, $T = \mu_o J^2 \left[\ell n(r_a/r_c) + 3/4 \right] /4\pi$, to be 62 nt, The latter component, calculated by assuming the measured chamber pressure of 0.02 atm acts over the entire anode orifice, is 16 nt making a total thrust of 78 nt. Integration of the measured impact pressure profile, which should also give the total thrust, yields 81 nt in good agreement with the calculated sum of the components. Similar agreement was obtained at the other mass flows and currents indicating all major sources and sinks of momentum in the MPD exhaust have been identified.

IV. SELECTION OF OTHER PROGRAMS IN PROGRESS

A. Hollow-Cathode, Quasi-Steady MPD Arc (Parmentier)

It has been experimentally demonstrated that substantial benefits accrue from the use of a hollow cathode for currents below 10A.[IV-1,IV-2] When the operating conditions and geometry are proper, a stable discharge originates inside the cathode cavity resulting in a lower cathode fall voltage, lower radiation losses, and less erosion. The object of the present study is two-fold: first, to investigate whether a hollow cathode will operate in the multi-megawatt power range typical of quasi-steady MPD arcs; and second, if this operation can be demonstrated, to determine whether the benefits observed at low powers are present at high powers as well.

Earlier tests with a cylindrical hollow cathode[119] showed that under some test conditions, the total arc impedance decreased, while for others, the impedance increased. In addition, Kerr-cell photographs showed little evidence that the discharge was emanating from the cathode cavity. In recent tests, two stainless steel hollow cathodes were employed. The first, Fig.IV-1a, is a conical configuration of overall dimensions similar to our solid conical cathodes. The motivation for this design is that the arc attachment at the cathode tip should generate a sufficiently large magnetic pressure to overcome the gasdynamic pressure associated with the mass flow through the cathode, and force the current attachment back into the cavity. The second cathode, Fig.IV-1b, is a larger diameter open configuration with nylon covering both the outer cylindrical surface and the downstream face. With this design, the discharge is forced to attach somewhere on the inner cylindrical surface.

The cathodes were tested in our standard MPD chamber configuration with the current pulse supplied by an electrolytic capacitor bank and the mass flow provided by the now standard

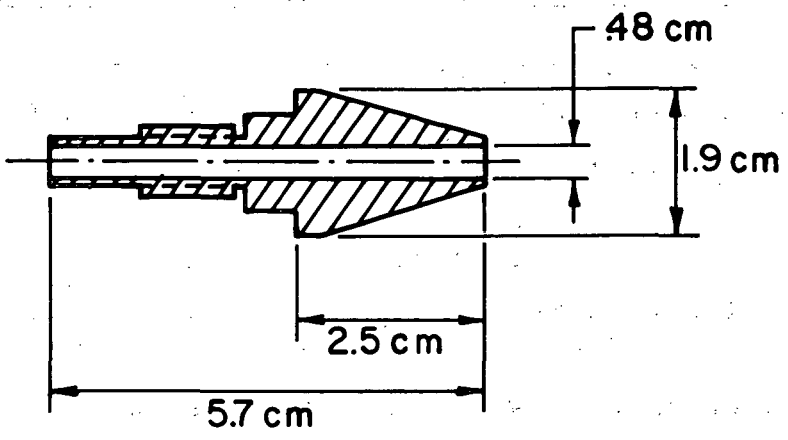

a) CONICAL HOLLOW CATHODE

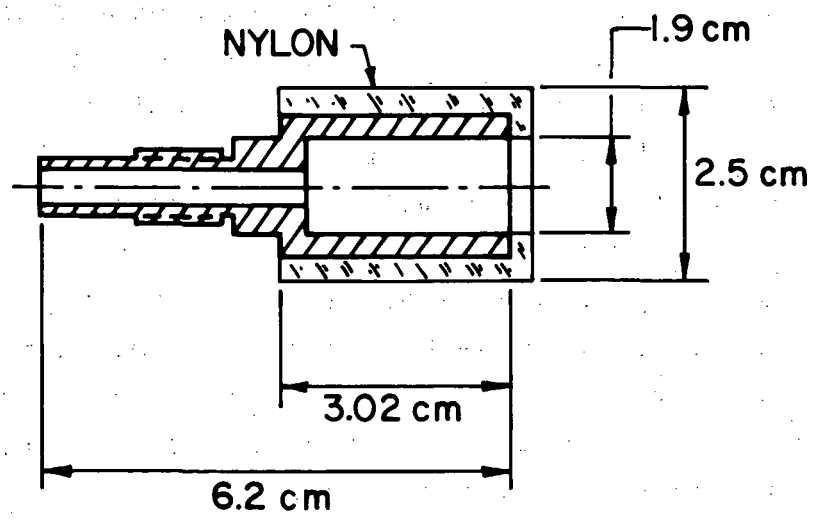

b) INSULATED HOLLOW CATHODE

CATHODE CONFIGURATIONS

FIGURE IV-1
AP 25-4729

electromagnetic solenoid valve. A small manifold mounted directly behind the arc chamber split the flow between the six normal chamber injectors and the cathode feed tube. Various orifices were inserted in these feed lines to change the fraction of the total mass flow which passes through the cathode.

Voltage data for these two cathodes, acquired over a large range of current, mass flow, and percentage distribution of mass flow, showed the insulated cathode to have the greater effect and thus, only these data will be presented. Although wide in scope, the data must be considered strictly preliminary due to the limited number of shots taken. Consequently, interpretation of and conclusions drawn from these data will be deferred until the trends have been fully verified.

A typical voltage-current discharge characteristic for a mass flow of 2.1 g/sec argon and a representative division of the flow of 67% through the chamber injectors and 33% through the inside of the cathode is shown in Fig.IV-2. This type of characteristic has been observed over the complete spectrum of flow division percentages for the same total mass flow, a summary of which is shown in Fig.IV-3. Also shown in the figure is one possible set of lines through these data for fixed current levels for the purpose of representing performance trends. For a fixed terminal voltage and a fixed flow division between chamber injectors and cathode, the measured current as a function of argon mass flow is shown in Fig.IV-4. The appearance of a maximum current followed by a plateau as mass flow is increased is borne out for other voltages and flow divisions.

These trends are summarized in Fig.IV-5, where the mass flow is plotted against percent division of the flow for several values of current and a fixed terminal voltage of 220 volts. For a fixed percentage flow inside, the data indicate that there are two different injected flow rates where the power input into the discharge is the same. Stated in another way, there is an optimum mass flow rate (defined as the maximum current for a fixed voltage) for any given distribution of the flow between

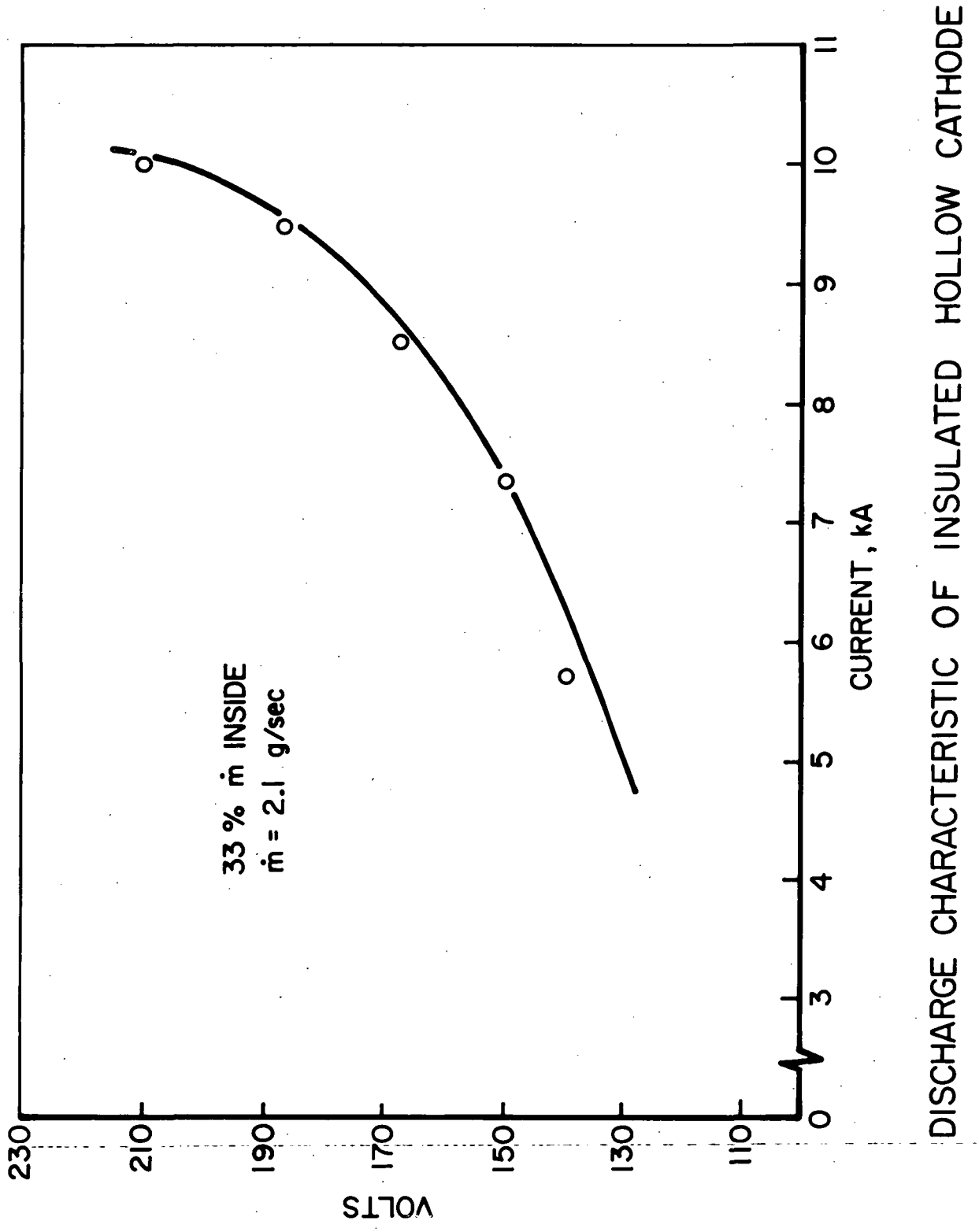

FIGURE IV-2
AP25-4727

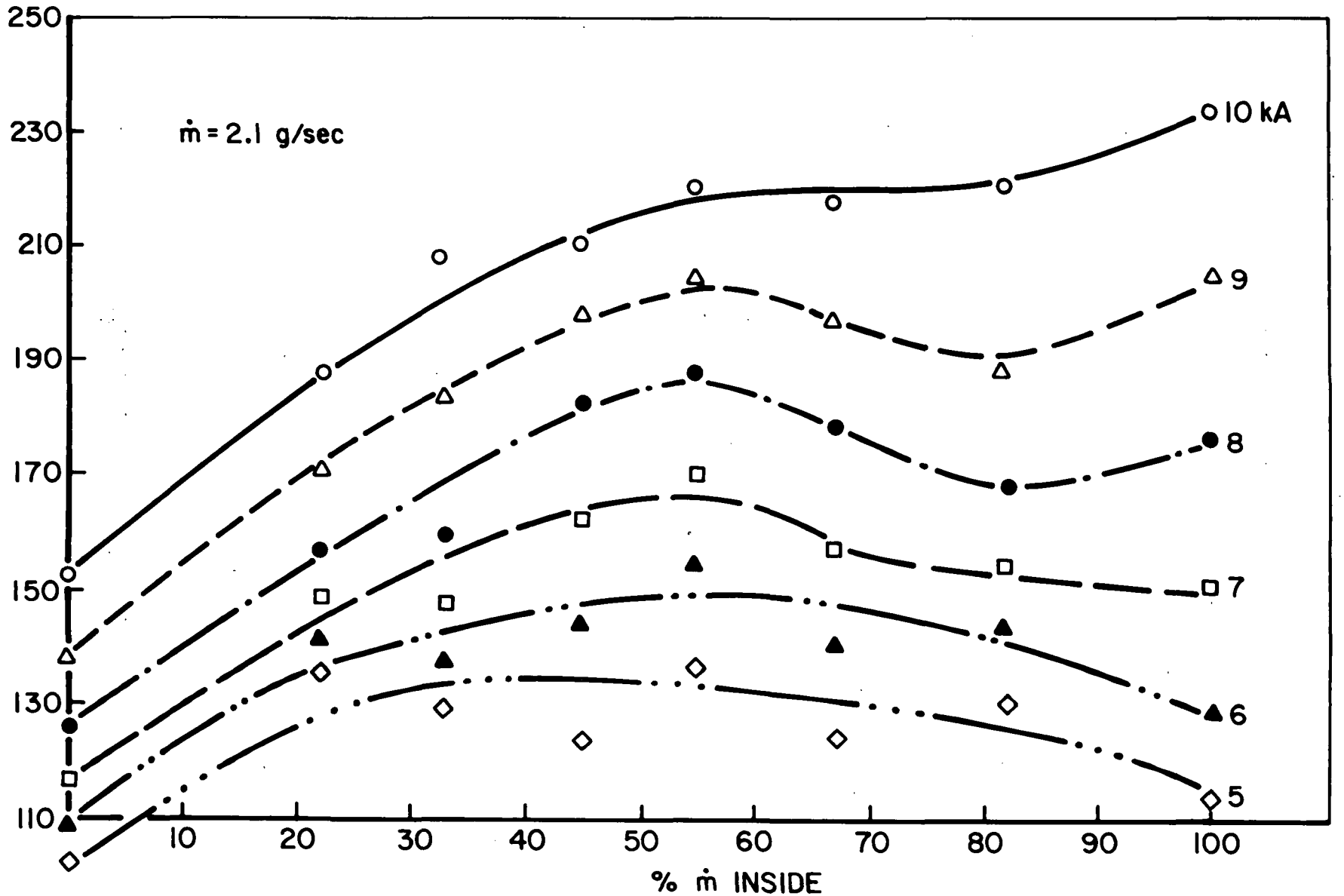

FIGURE IV-3
AP25-4726

SUMMARY OF DISCHARGE CHACTERISTICS OF INSULATED HOLLOW CATHODE

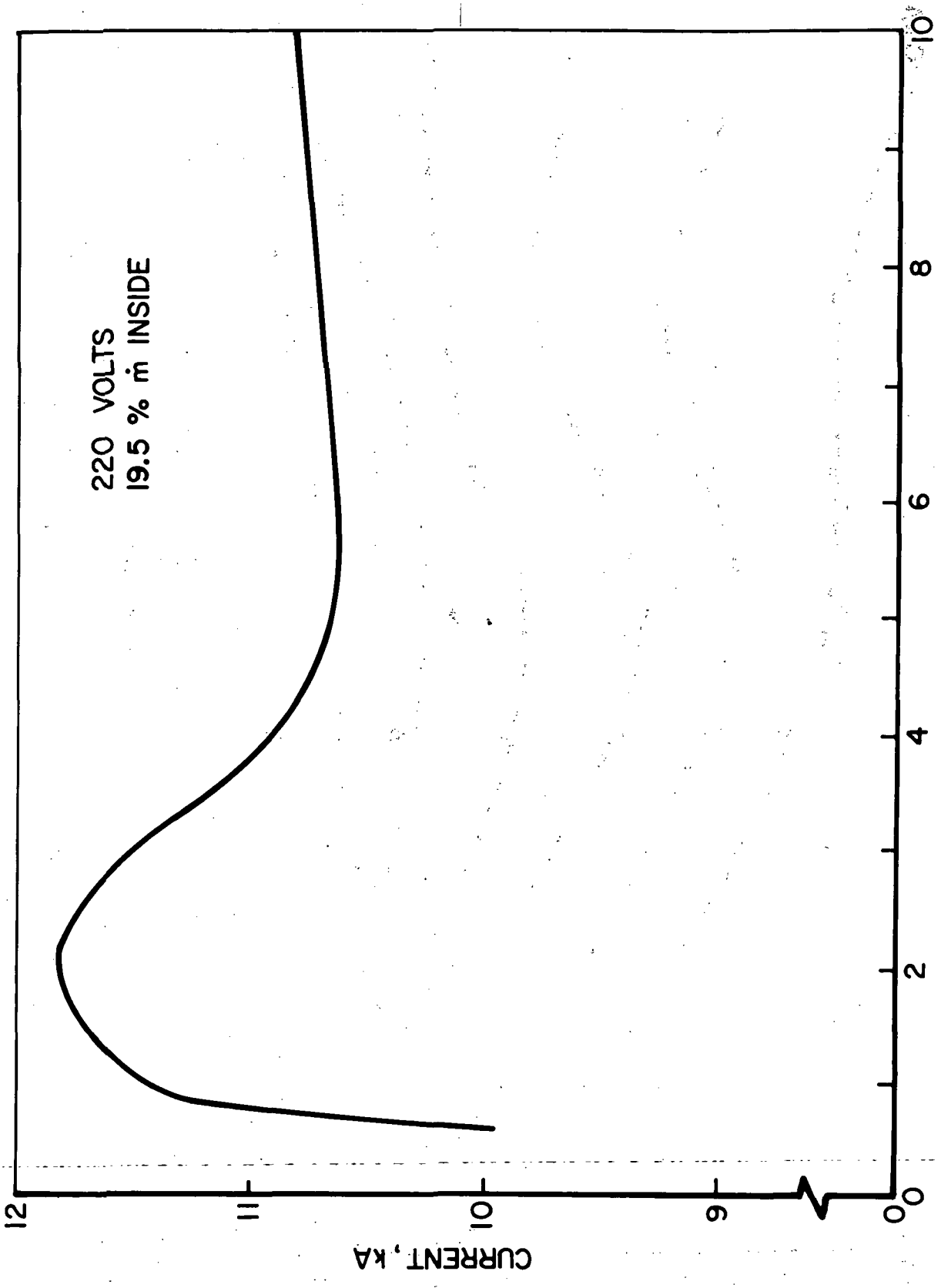

DISCHARGE CURRENT-MASS FLOW CHARACTERISTIC
OF INSULATED HOLLOW CATHODE

FIGURE IV-4
AP25-4725

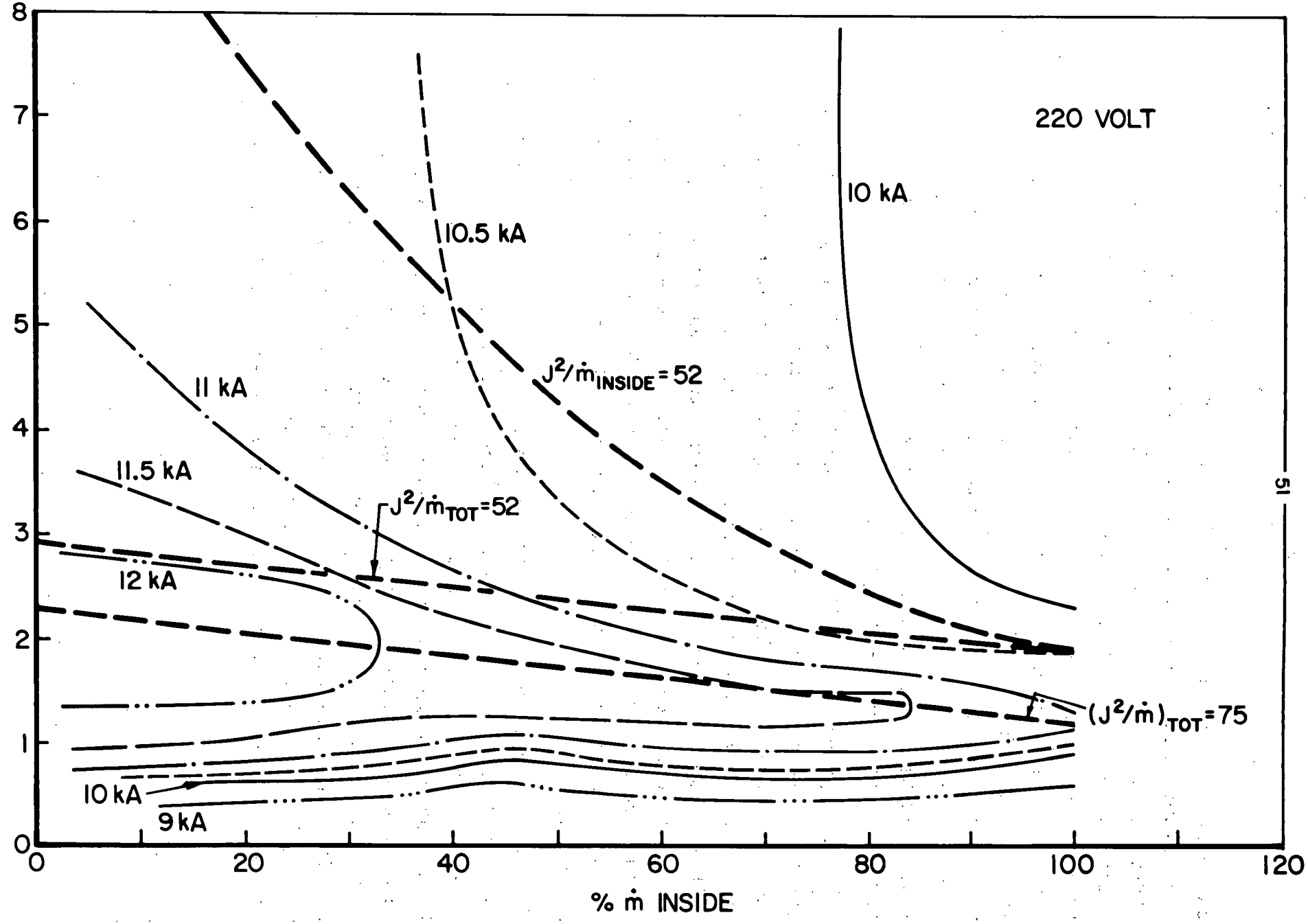

FIGURE IV-5
AP 25-4723

DISCHARGE MASS FLOW CHARACTERISTICS
OF INSULATED HOLLOW CATHODE

outer injectors and the cathode. The locus of these optimum mass flows coincides with a line of constant $J^2/\dot{m}$, the constant equal to 75 for these particular data. For comparison, a line of $J^2/\dot{m} = 52$ has also been drawn which is the characteristic value calculated for this geometry from a simple argument based on an equipartition of energy between kinetic and thermal modes. [IV-3] A similar line drawn for $J^2/\dot{m} = 52$, where $\dot{m}$ is only that mass passing through the cathode, seems to bear little relation to any of the key features of the figure emphasizing that the total mass flow is a better scaling parameter for these terminal data.

Data points which lie above the $J^2/\dot{m} = 75$, i.e. mass flows greater than the optimum value, may indicate an overfed region whereas those below the line may represent a region of starvation. Thus, the apparent insensitivity of the data to the initial flow distribution at low mass flows may be a manifestation of electrode or insulator erosion at these conditions. In support of a starvation argument, the front face of the cathode and insulator were severely eroded after this series of shots.

To minimize this erosion and to investigate these trends in more detail, a new tungsten hollow cathode has been installed in the discharge chamber. The cathode is larger, 3.2 cm in diameter, to facilitate probing of the interior in order to determine what fraction of the discharge current is emanating from the cavity, and to allow better photographic observation. In addition, this configuration will be driven by one of our high voltage capacitor lines instead of the electrolytic line to insure a flat current pulse at a predetermined level.

B. Time-Resolved Thrust Measurement (Saber)

Recent experiments have shown the first positive results of a thrust-time profile measured with piezoresistive strain gauges mounted on structural elements of a quasi-steady MPD accelerator. Initial tests revealed that the response of individual gauges mounted on the inside of the cathode cylinder was dominated by both electrical and mechanical noise. The electrical noise is now reduced to a tolerable level by the various techniques illustrated in Fig. IV-6. Most of the electromagnetic pickup is eliminated by differentially monitoring the output of two identical strain gauges, one mounted on the cathode cylinder and a second passive gauge suspended directly above it. Careful shielding of this sandwich structure as well as the rest of the bridge circuit leads to a noise level of 0.1 mv compared to an anticipated signal level of the order of 1 mv. Mechanical pickup by the sensor was primarily related to initiation of the mass flow in the shock tube mass injection system. This source of noise was temporarily eliminated by operating in the "ambient" mode, i.e. prefilling the entire Plexiglas vacuum tank to a fixed pressure level, say 100 μ, and firing the accelerator without further injection of any mass. This problem will be permanently resolved when the electromagnetic valve mass injection system is in standard use.

Fig. IV-7 shows the response of the strain gauge to a 40 kA x 0.5 msec current pulse on three different time scales. The 50 μsec delay before the initial gauge response is due to the finite propagation time of the strain wave down the cathode cylinder, but also illustrates the low noise level compared to the data signal. After 50 μsec, the trace displays a superposition of two characteristic frequencies on the data signal - a 10 kHz pattern corresponding to the propagation and reflection of the longitudinal strain wave in the cathode cylinder, and a 1 kHz wave corresponding to a "drumhead" oscillation of the cathode end plate. These oscillations are more clearly shown in Fig. IV-8

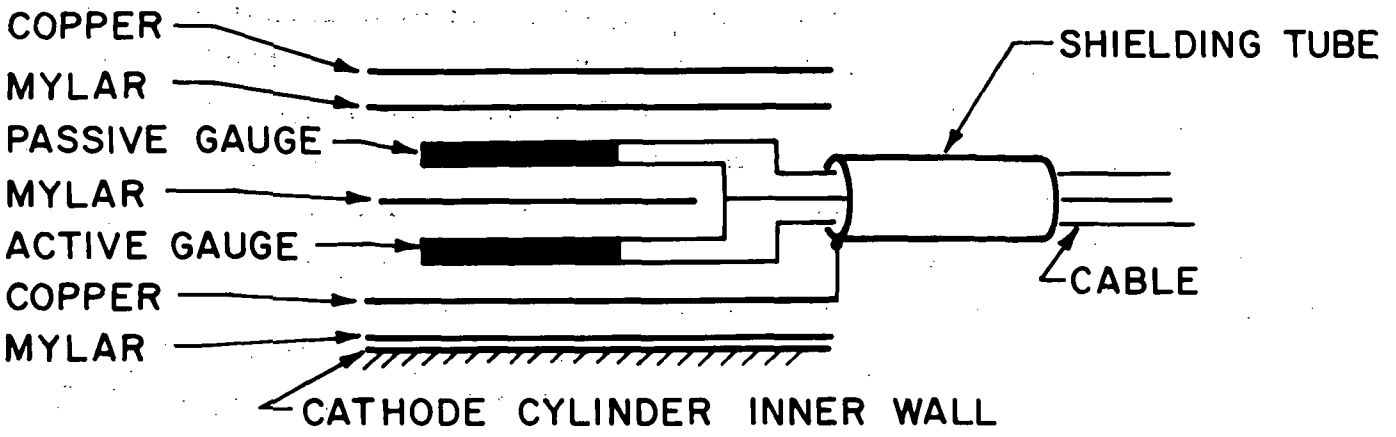

a) STRAIN GAUGE ASSEMBLY

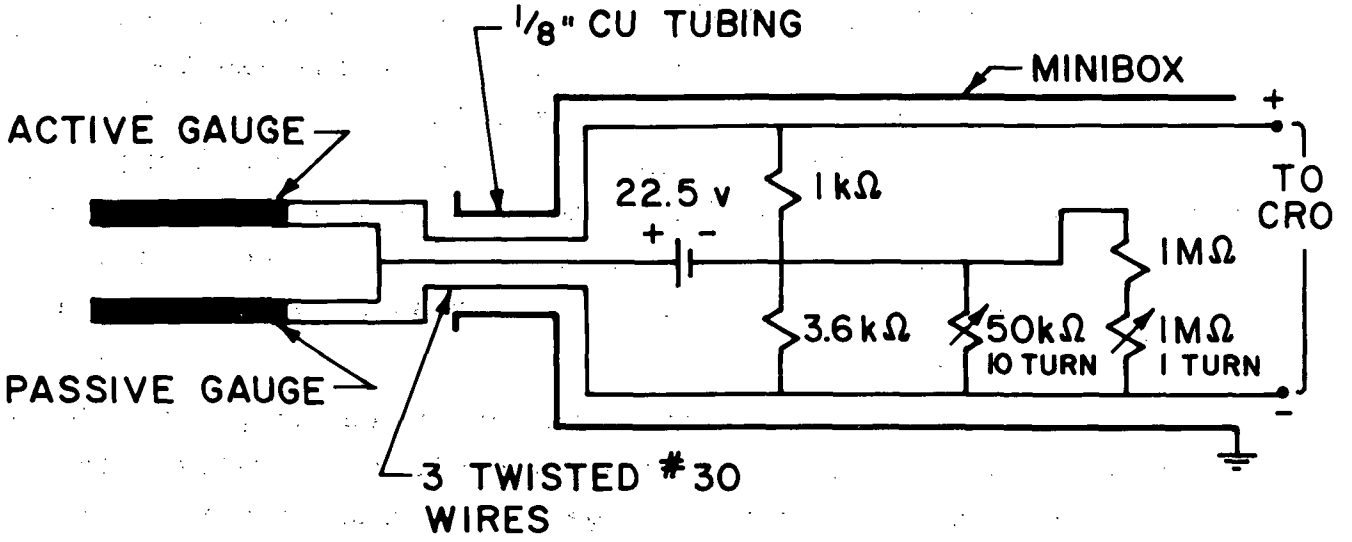

b) SCHEMATIC OF BRIDGE CIRCUIT

STRAIN GAUGE THRUST TRANSDUCER SYSTEM

FIGURE IV-6
AP25-4735

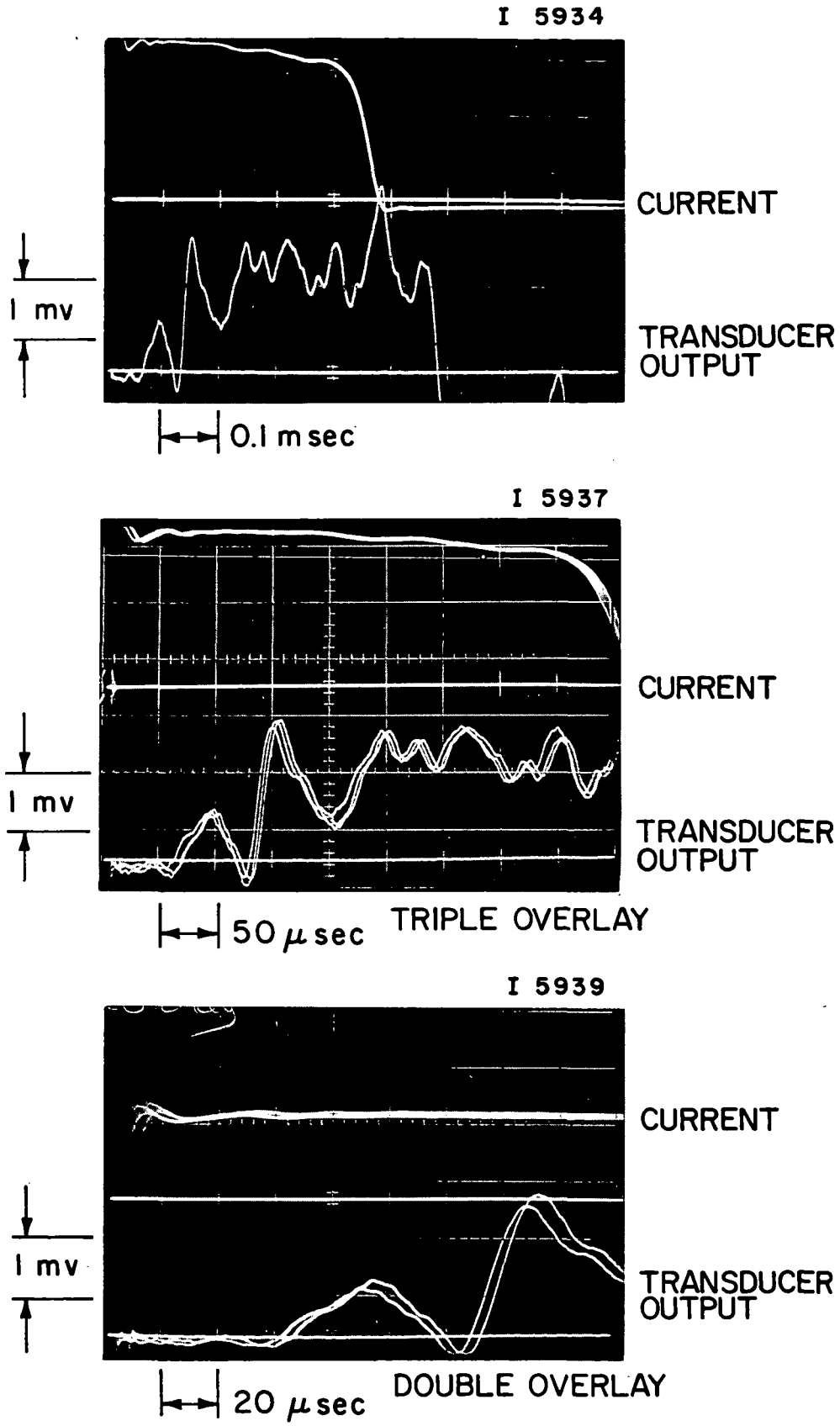

STRAIN GAUGE SYSTEM OUTPUT
40 kA - ½ m sec DURATION

FIGURE IV-7
AP25-P375

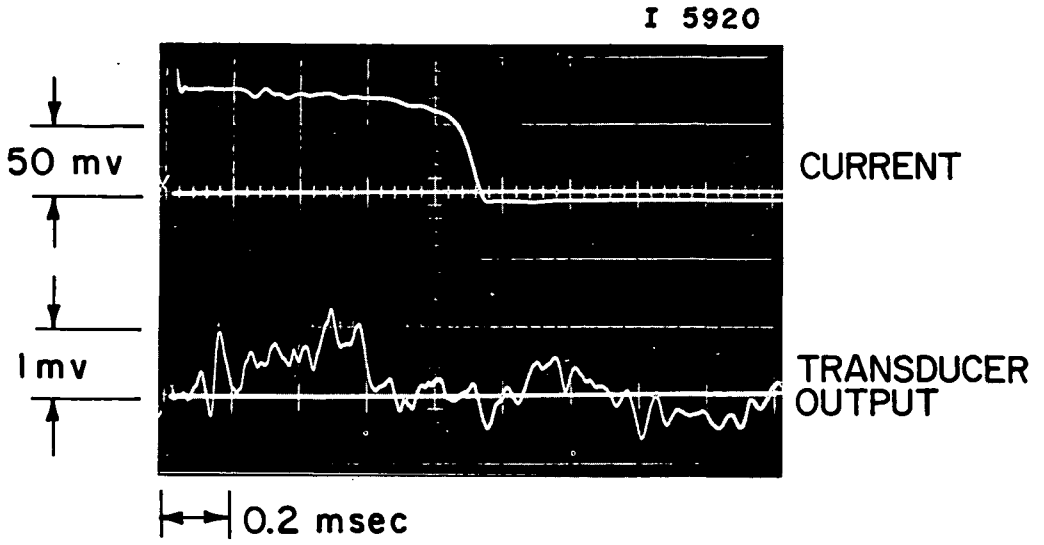

FORWARD CURRENT-21.5 kA, 1msec DURATION

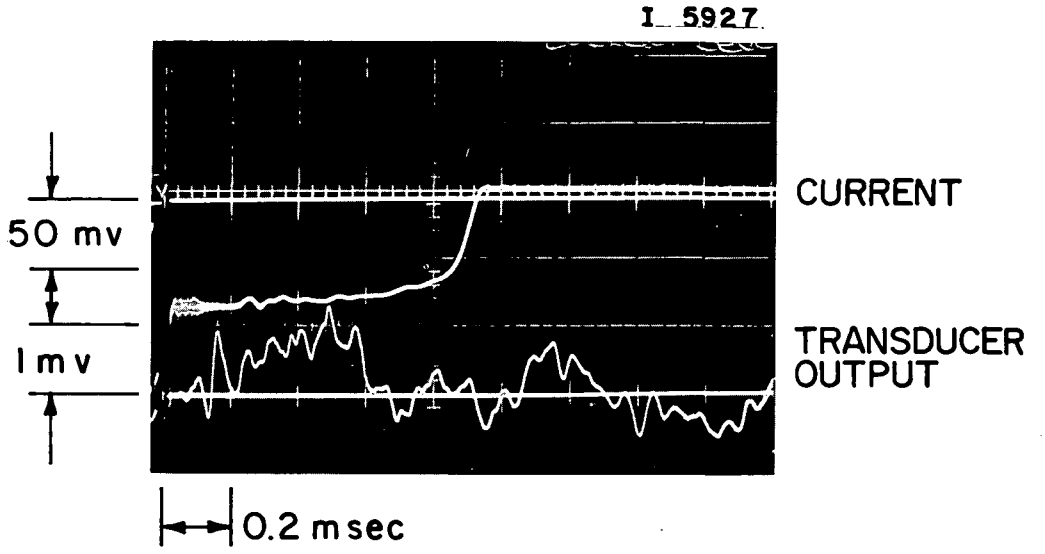

REVERSED CURRENT-21.5 kA, 1msec DURATION

FORWARD AND REVERSED CURRENT COMPARISON

FIGURE IV-8
AP25-P372

where the gauge response to both a forward and reversed 21.5 kA x 1 msec current pulse is shown. Since the thrust is almost completely generated by the interaction of the current with its own magnetic field, current reversal should have no effect on this electromagnetic thrust component as long as the current distribution remains azimuthally symmetric. As seen in Fig. IV-8 there is no discernible difference in the transducer output for these conditions indicating that the observed signal is both free of spurious noise and representative of an electromagnetic thrust record.

Further evidence that the gauge is responding to electromagnetic thrust is presented in Fig. IV-9. As the current is raised by approximately 75%, the amplitude of the initially excited strain waves increases by approximately the square of this current change. Thus, although the mechanics of the accelerator deformation complicate the extraction of the true thrust level, the strain gauge technique appears to be a viable one for recording thrust-time profiles in this hostile environment.

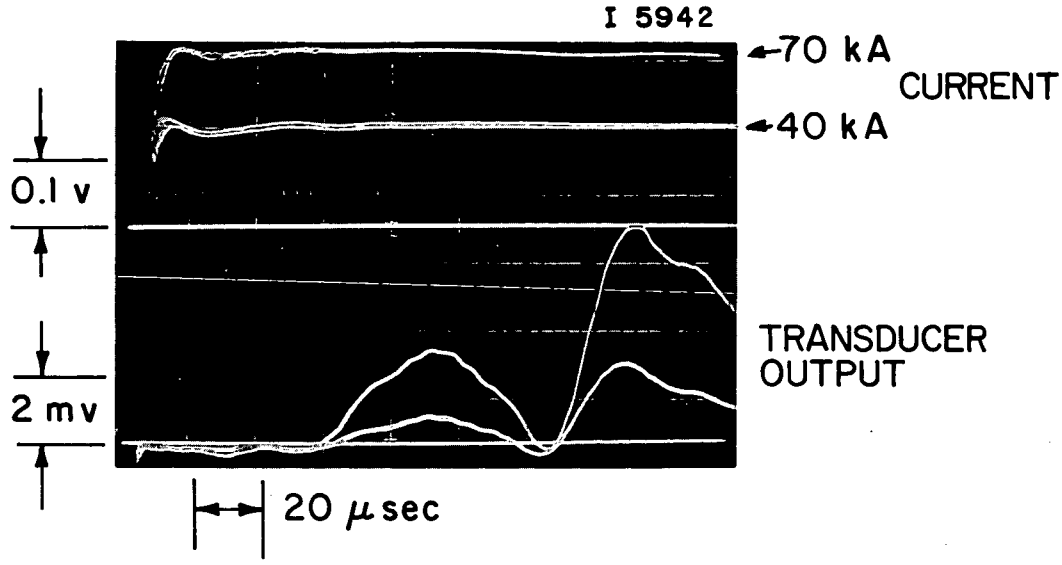

SIGNAL AT 40 kA AND 70 kA

FIGURE IV-9
AP25-P376

C. Time-of-Flight Velocity Probes (Boyle)

Signals from double electric probes biased to draw ion saturation current have been previously used in this laboratory to determine plasma velocity profiles in the exhaust of an MPD accelerator.[85,97,118] If one assumes that the microstructure of the velocity probe signal is characteristic of fluctuations in local plasma properties and that these fluctuations convect with the streaming motion of the exhaust flow, then the plasma velocity can be readily obtained from a time-of-flight measurement based on correlation of the signals from two of these probes displaced a known axial distance.

A program has been initiated to investigate the accuracy of the calculated plasma velocity based upon the time-of-flight hypothesis. Theoretical support for the program is based on collisionless probe theory for the cylindrical Langmuir probe in a stationary Maxwellian plasma by Laframboise.[IV-4] When such a cylindrical probe is aligned at an angle to the incident plasma flow, the probe current is found to be a function of local plasma properties, plasma velocity, probe bias, and ratio of probe radius to Debye length. Since the local electron number density, electron temperature and ion temperature have been previously determined in the MPD exhaust,[111,118,119] such a probe should yield the plasma velocity from the experimentally determined voltage-current characteristic and probe geometry. Thus, a time-of-flight probe consisting of two of these cylindrical probes provides data for three independently calculated velocities - two from the individual probe characteristics via probe theory and one directly from convective fluctuations. Agreement among these velocities establishes the validity of the time-of-flight hypothesis on a physical basis.

As a first step in this program, a double probe has been constructed from 0.076-mm diameter tungsten wire. The electrodes are each 7.6 mm long with a 1 mm separation. For reasonable estimates of local plasma properties, the electron-electron,

electron-ion and ion-ion mean free paths are greater than the radius of the probe electrodes implying a collisionless flow regime. A length-to-diameter ratio of 100 assures end effects are negligible.[IV-5] The dimensions of the previously used parallel plate boundary layer probes were such that the probe operated in a transition flow regime, a difficult one to describe analytically.

Initial tests with this probe in the MPD exhaust indicate a similarity between the recorded currents of the collisionless probe and the previous parallel plate probe. For example, arrival times for the initial plasma front of approximately 8000 m/s are recorded, and the later quasi-steady portion of the signal has high frequency current fluctuations superimposed on it enabling convective fluctuation measurements to be made. As a result, a second cylindrical double probe has been constructed and voltage-current characteristics are now being recorded to evaluate the plasma velocity.

D. Repetitive Pulse Propellant Injection (White)

As the quasi-steady propulsion concept continues to evolve toward a working space thruster, increased attention must be directed toward various other components of the complete thruster system. The two areas of most concern involve the power preparation and gas injection subsystems. Of these, the conversion of DC solar power into intermittent, high current, square pulses is reasonably straightforward, with the primary task that of improving capacitor quality. On the other hand, the conversion of a high pressure, stored working fluid into 10^7 - 10^8 discrete mass pulses with stringent requirements on pulse rise time and shape, and minimum leakage between pulses has less evident technological solution. Conventional valves are too slow; valves that are overdriven to improve their rise time have questionable lifetime and reliability. In an effort to initiate some interest in this aspect of the problem, and to contribute to its solution, we have undertaken a program of repetitive-pulse gas injection which explicitly eschews reciprocating valves.

The most promising concept identified so far replaces the impulsively started and stopped member in conventional valves with a purely rotational system running at constant speed, where the seals will absorb far less energy, hence wear less. A prototype of this turbo-gas injector scheme has been designed, constructed, and tested which can deliver argon pulses of several grams per second, in a range of pulse lengths and separations. The device, shown in Fig. IV-10 consists of two coaxial slotted discs housed in an appropriate support and manifold assembly, and rotating at different angular velocities. Argon propellant, fed into a small plenum directly behind the discs, passes through the valve only when the slots become coincident. The gas pulse density profile in time is determined by the absolute speed of the fastest disc A in Fig. IV-10, which is coupled directly to a conventional electric motor; the dead time between gas pulses

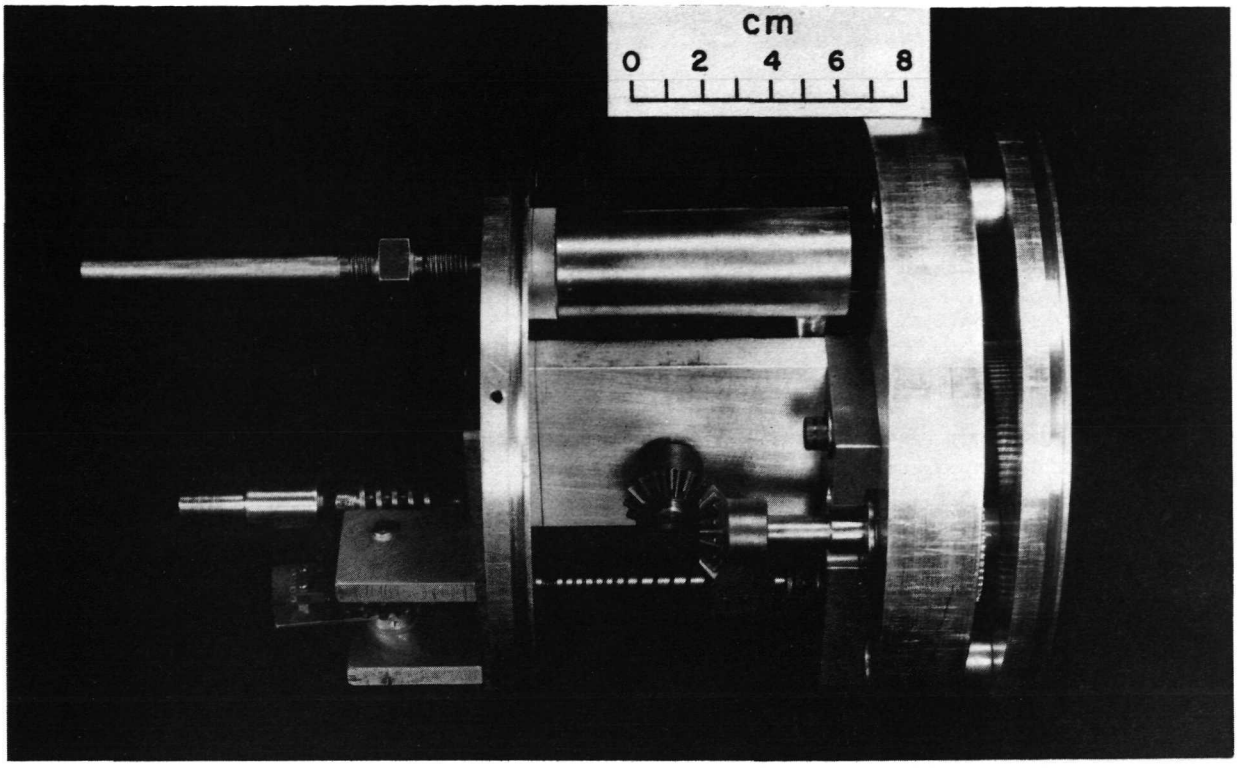

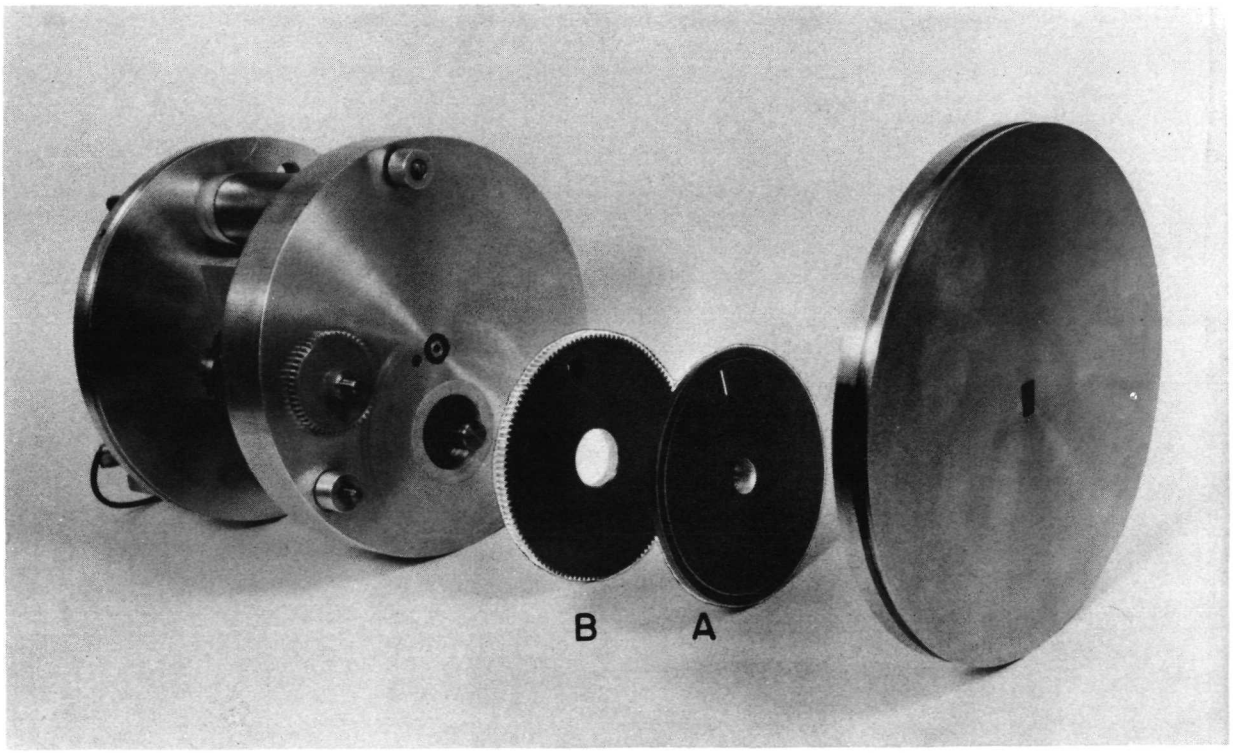

MULTIPLE PULSE PROPELLANT VALVE

FIGURE IV-10
AP25·P349

is fixed by the relative speeds of the two discs, with the slower disc B geared down from the high speed shaft. Thus, varying the motor speed, gear ratio between the discs, and number of holes in the slower disc allows this system to satisfy a wide range of pulse demands. For example, the lower line in Fig. IV-11 shows the anticipated operating range of pulse length and pulse frequency available to the prototype valve for a fixed gear ratio of 24:1 and a single slot in the slow disc. Operation along the line is possible by varying the speed of the driving motor. The 10^{-3} duty cycle (ratio of on-time to total on-time plus off-time), which exists for all operating conditions along this line, is a consequence of the gear ratio, slot dimensions, and the single slot in the slow disc. Other operating lines accessible by increasing the number of slots in the low-speed disc are shown in the figure along with their respective duty cycles.

For the initial testing of this valve, the rotation rate was set at 1725 rpm which should ideally produce 0.83 msec pulses with a risetime of 83 μsec, at a repetition rate of 1.2 pulses per second. Figure IV-12 shows the density profile for these pulses as recorded by a Millitorr fast ionization gauge a few cm in front of the exit orifice. The lower trace shows that a single pulse occurs approximately every 0.8 sec as expected with no significant leakage during the dead time. The detailed profiles of each of the six pulses shown in the lower trace are overlaid in the upper trace on an expanded time scale. Although the starting transient is not ideal, the bulk of the pulse has a risetime of roughly 200 μsec. These reproducible data are highly encouraging in that they indicate rise and fall times and pulse durations close to design values and considerably shorter than hybrid solenoid valve systems.

The ripple or "false start" observed at the beginning of the pulse is apparently caused by improper initial alignment of the two discs. To improve this overall starting

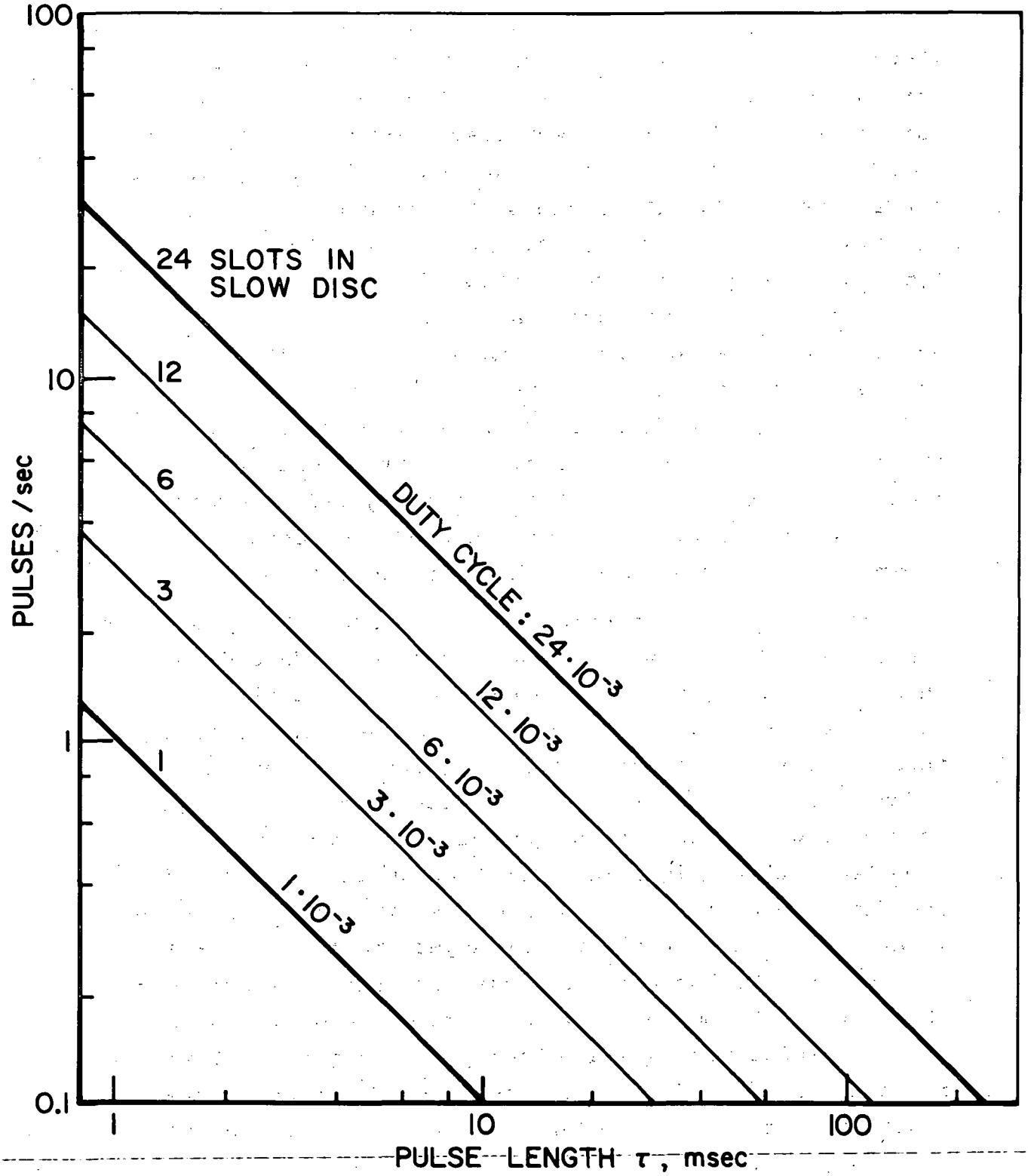

VALVE OPERATING RANGE

FIGURE IV-11
AP25·4724

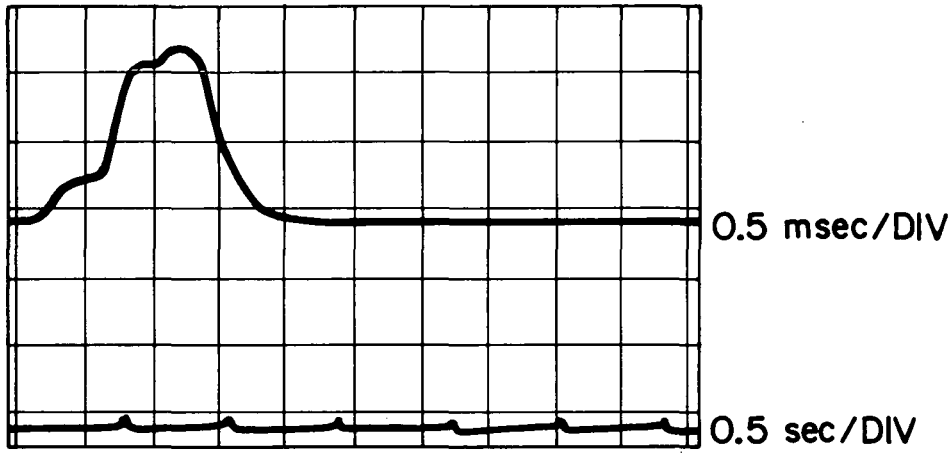

DENSITY PROFILE OF PROPELLANT PULSE

FIGURE IV-12
AP 25-4728

transient, a mechanical linkage will be added to the valve to allow continuous adjustment of the disc coincidence during operation. In addition, both discs will be Teflon coated to reduce friction and wear. Further testing should indicate the full range of deliverable gas pulses, long-term wear rates, and the compatability of this system with the discharge.

PROJECT REFERENCES

[1]Jahn, R. G., Bernstein, I. B. and Kunen, A. E., "Proposed Studies of the Formation and Stability of an Electromagnetic Boundary in a Pinch," Proposal for NASA Research Grant NsG-306-63, Mar. 5, 1962, Princeton Univ., Princeton, N. J.

[2]Jahn, R. G. and von Jaskowsky, W. F., "Pulsed Electromagnetic Gas Acceleration," NASA NsG-306-63 progress report for the period 1 July 1962 to 31 December 1962, Aeron. Eng. Rept. No. 634, Jan. 1963, Princeton Univ., Princeton, N. J.

[3]Jahn, R. G. and von Jaskowsky, W. F., "The Plasma Pinch as a Gas Accelerator," A.I.A.A. Preprint 63013, A.I.A.A. Electric Propulsion Conference, Colorado Springs, Colo., 11-13 Mar. 1963.

[4]Jahn, R. G. and von Jaskowsky, W. F., "Pulsed Electromagnetic Gas Acceleration," NASA NsG-306-63 progress report for the period 1 January 1963 to 30 June 1963, Aeron. Eng. Report No. 634a, June 1963, Princeton Univ., Princeton, N. J.

[5]Jahn, R. G. and von Jaskowsky, W. F., "Structure of a Large-radius Pinch Discharge," A.I.A.A. Journal, Vol. 1, No. 8, Aug. 1963, pp. 1809-1814.

[6]Jahn, R. G., von Jaskowsky, W. F. and Casini, A. W., "A Gas-triggered Inverse Pinch Switch," NASA NsG-306-63, Aeron. Eng. Tech. Note No. 660, Aug. 1963, Princeton Univ., Princeton, N. J.

[7]Jahn, R. G., von Jaskowsky, W. F. and Casini, A. L., "Gas triggered Inverse Pinch Switch," The Review of Scientific Instruments, Vol. 34, No. 12, Dec. 1963, pp. 1439-1440.

[8]Jahn, R. G. and von Jaskowsky, W. F., "Pulsed Electromagnetic Gas Acceleration," (Paper delivered at the 4th NASA Intercenter Conference on Plasma Physics, Washington, D. C., 2-4 Dec. 1963), p. 8.

[9]Jahn, R. G. and von Jaskowsky, W. F., "Pulsed Electromagnetic Gas Acceleration," NASA NsG-306-63 progress report for period 1 July 1963 to 31 December 1963, Aeron. Eng. Rept. No. 634b, Dec. 1963, Princeton Univ., Princeton, N. J.

PROJECT REFERENCES

[10]Jahn, R. G. and von Jaskowsky, W. F., "Current Distributions in Large-radius Pinch Discharges," A.I.A.A. Preprint 64-25, A.I.A.A. Aerospace Sciences Meeting, New York, N. Y., 20-22 Jan. 1964.

[11]Jahn, R. G. and von Jaskowsky, W. F., "Current Distributions in Large-radius Pinch Discharges," A.I.A.A. Bulletin, Vol. 1, No. 1, Jan. 1964, p. 12.

[12]Jahn, R. G. and von Jaskowsky, W. F., "Pulsed Electromagnetic Gas Acceleration," NASA NsG-306-63 renewal proposal for 15-months extension, Jan. 15, 1964, Princeton Univ., Princeton, N. J.

[13]Jahn, R. G. and von Jaskowsky, W. F., "Pulsed Electromagnetic Gas Acceleration," NASA NsG-306-63 progress report for the period 1 January 1964 to 30 June 1964, Aeron. Eng. Rept. No. 634c, July 1964, Princeton Univ., Princeton, N. J.

[14]Jahn, R. G., von Jaskowsky, W. F. and Casini, A. L., "Gas-triggered Pinch Discharge Switch," NASA NsG-306-63, Aerospace and Mechanical Sciences Tech. Note No. 101, July 1964, Princeton Univ., Princeton, N. J.

[15]Corr, J. M., "Double Probe Studies in an 8" Pinch Discharge," M.S.E. thesis, Sept. 1964, Princeton Univ., Princeton, N. J.

[16]Jahn, R. G. and von Jaskowsky, W. F., "Exhaust of a Pinched Plasma From an Axial Orifice," A.I.A.A. Bulletin, Vol. 1, No. 10, Oct. 1964, p. 570.

[17]Jahn, R. G. and von Jaskowsky, W. F., "Current Distributions in Large-radius Pinch Discharges," A.I.A.A. Journal, Vol. 2, No. 10, Oct. 1964, pp. 1749-1753.

[18]Jahn, R. G., von Jaskowsky, W. F. and Casini, A. L., "Gas-triggered Pinch Discharge Switch", The Review of Scientific Instruments, Vol. 36, No. 1, Jan. 1964, pp. 101-102.

[19]Jahn, R. G. and von Jaskowsky, W. F., "Exhaust of a Pinched Plasma from an Axial Orifice," A.I.A.A. Paper 65-92, A.I.A.A. 2nd Aerospace Sciences Meeting, New York, N. Y., 25-27 Jan. 1964.

PROJECT REFERENCES

[20]Jahn, R. G. and von Jaskowsky, W. F., "Pulsed Electromagnetic Gas Acceleration," NASA NsG-306-63 progress report for the period 1 July 1964 to 31 December 1964, Aerospace and Mechanical Sciences Rept. No. 634d, Jan. 1965, Princeton Univ., Princeton, N. J.

[21]Wright, E. S., "The Design and Development of Rogowski Coil Probes for Measurement of Current Density Distribution in a Plasma Pinch," M.S.E. thesis, May 1965, Princeton Univ., Princeton, N. J.

[22]Jahn, R. G. and von Jaskowsky, W. F., "Pulsed Electromagnetic Gas Acceleration," NASA NsG-306-63 renewal proposal for 12-months extension, June 7, 1964, Princeton Univ., Princeton, N. J.

[23]Jahn, R. G. and Black, N. A., "On the Dynamic Efficiency of Pulsed Plasma Accelerators," A.I.A.A. Journal, Vol. 3, No. 6, June 1965, pp. 1209-1210.

[24]Black, N. A., "Linear Pinch Driven by a High-current Pulse-forming Network," A.I.A.A. Bulletin, Vol. 2, No. 6, June 1965, p. 309.

[25]Wright, E. S. and Jahn, R. G., "The Design and Development of Rogowski Coil Probes for Measurement of Current Density Distribution in a Plasma Pinch," NASA NsG-306-63, Aerospace and Mechanical Sciences Rept. No. 740, June 1965, Princeton Univ., Princeton, N. J.

[26]Rowell, G. A., "Cylindrical Shock Model of the Plasma Pinch," M.S.E. thesis, July 1965, Princeton Univ., Princeton, N. J.

[27]Black, N. A., "Linear Pinch Driven by a High-current Pulse-forming Network," A.I.A.A. Paper 65-336, A.I.A.A. 2nd Annual Meeting, San Francisco, Calif., 26-29 July 1965.

[28]Jahn, R. G. and von Jaskowsky, W. F., "Pulsed Electromagnetic Gas Acceleration," NASA NsG-306-63 progress report for the period 1 January 1965 to 30 June 1965, Aerospace and Mechanical Sciences Rept. No. 634e, July, 1965, Princeton Univ., Princeton, N. J.

[29]Jahn, R. G. and Ducati, A. C., "Design and Development of a Thermo-Ionic Electric Thrustor," 5QS 085-968 Interim Report, NASA Contract NASw-968, Aug. 1965, Giannini Scientific Corp., Santa Ana, Calif.

PROJECT REFERENCES

[30]Jahn, R. G., von Jaskowsky, W. F. and Burton, R. L., "Ejection of a Pinched Plasma From an Axial Orifice," A.I.A.A. Journal, Vol. 3, No. 10, Oct. 1965, pp. 1862-1866.

[31]Jahn, R. G. and Wright, E. S., "Miniature Rogowski Coil Probes for Direct Measurement of Current Density Distribution in Transient Plasmas," The Review of Scientific Instruments, Vol. 36, No. 12, Dec. 1965, pp. 1891-1892.

[32]Jahn, R. G. and von Jaskowsky, W. F., "Pulsed Electromagnetic Gas Acceleration," NASA NsG-306-63 progress report for the period 1 July 1965 to 31 December 1965, Aerospace and Mechanical Sciences Rept. No. 634f, Jan. 1966, Princeton Univ., Princeton, N. J.

[33]Burton, R. L. and Jahn, R. G., "Electric and Magnetic Field Distributions in a Propagating Current Sheet," A.I.A.A. Bulletin, Vol. 3, No. 1, Jan. 1966, p. 35.

[34]Rowell, G. A., Jahn, R. G. and von Jaskowsky, W. F., "Cylindrical Shock Model of the Plasma Pinch," NASA NsG-306-63, Aerospace and Mechanical Sciences Rept. No. 742, Feb. 1966, Princeton Univ., Princeton, N. J.

[35]Burton, R. L. and Jahn, R. G., "Electric and Magnetic Field Distributions in a Propagating Current Sheet," A.I.A.A. Paper 66-200, A.I.A.A. 5th Electric Propulsion Conference, San Diego, Calif., 7-9 Mar. 1966.

[36]Black, N. A., "Pulse-forming Networks for Propulsion Research," Proceedings of the 7th Symposium on Engineering Aspects of Magnetohydrodynamics, Princeton Univ., Princeton, N. J., Mar. 30-April 1, 1966, pp. 10-11.

[37]Jahn, R. G., "Electromagnetic Propulsion," Astronautics and Aeronautics, Vol. 4, No. 4, April 1966, p. 69.

[38]Black, N. A., "Dynamics of a Pinch Discharge Driven by a High-current Pulse-forming Network," Ph.D. thesis, May 1966, Princeton Univ., Princeton, N. J.

[39]Black, N. A. and Jahn, R. G., "Dynamics of a Pinch Discharge Driven by a High-current Pulse-forming Network," NASA NsG-306-63, Aerospace and Mechanical Sciences Rept. No. 778, May 1966, Princeton Univ., Princeton, N. J.

PROJECT REFERENCES

[40]Jahn, R. G., "Pulsed Plasma Propulsion," Proceedings of the 5th NASA Intercenter and Contractors Conference on Plasma Physics, Washington, D. C., 24-26 May 1966, pt. V, pp. 75-81.

[41]Jahn, R. G. and von Jaskowsky, W. F., "Pulsed Electromagnetic Gas Acceleration," NASA NsG-306-63 renewal proposal for 24-months extension, May 25, 1966, Princeton Univ., Princeton, N. J.

[42]Ducati, A. C., Jahn, R. G., Muehlberger, E. and Treat, R. P., "Design and Development of a Thermo-Ionic Electric Thrustor," FR-056-968 Final Report, NASA CR-54703, May 1966, Giannini Scientific Corp., Santa Ana, Calif.

[43]Jahn, R. G. and Clark, K. E., "A Large Dielectric Vacuum Facility," A.I.A.A. Journal, Vol. 4, No. 6, June 1966, p. 1135.

[44]John, R. R., Bennett, S. and Jahn, R. G., "Current Status of a Plasma Propulsion," A.I.A.A. Bulletin, Vol. 3, No. 5, May 1966, p. 264.

[45]John, R. R., Bennett, S. and Jahn, R. G., "Current Status of a Plasma Propulsion," A.I.A.A. Paper 66-565, A.I.A.A. 2nd Propulsion Joint Specialist Conference, Colorado Springs, Colo., 13-17 June 1966.

[46]Jahn, R. G. and von Jaskowsky, W. F., "Pulsed Electromagnetic Gas Acceleration," NASA NsG-306-63 progress report for the period 1 January 1966 to 30 June 1966, Aerospace and Mechanical Sciences Rept. No. 634g, July 1966, Princeton Univ., Princeton, N. J.

[47]Burton, R. L., "Structure of the Current Sheet in a Pinch Discharge," Ph.D. thesis, Sept. 1966, Princeton Univ., Princeton, N. J.

[48]Burton, R. L. and Jahn, R. G., "Structure of the Current Sheet in a Pinch Discharge," NASA NsG-306-63, Aerospace and Mechanical Sciences Rept. No. 783, Sept. 1966, Princeton Univ., Princeton, N. J.

[49]Jahn, R. G. and von Jaskowsky, W. F., "Pulsed Electromagnetic Gas Acceleration," NASA NsG-306-63 progress report for the period 1 July 1966 to 31 December 1966, Aerospace and Mechanical Sciences Rept. No. 634h, Jan. 1967, Princeton Univ., Princeton, N. J.

PROJECT REFERENCES

[50]Burton, R. L. and Jahn, R. G., "Structure of the Current Sheet in a Pinch Discharge," Bulletin of the American Physical Society, Vol. 12, Ser. II, Paper L1, May 1967, p. 848.

[51]Jahn, R. G., "Plasma Propulsion for Deep Space Flight," Bulletin of the American Physical Society, Vol. 12, Ser. II, Paper BC-1, May 1967, p. 646.

[52]Ellis, W. R., Jr., "An Investigation of Current Sheet Structure in a Cylindrical Z-Pinch," Ph.D. thesis, July 1967, Princeton Univ., Princeton, N. J.

[53]Ellis, W. R., Jr. and Jahn, R. G., "An Investigation of Current Sheet Structure in a Cylindrical Z-Pinch," NASA NsG-306-63, Aerospace and Mechanical Sciences Rept. No. 805, July 1967, Princeton Univ., Princeton, N. J.

[54]Jahn, R. G. and von Jaskowsky, W. F., "Pulsed Electromagnetic Gas Acceleration," NASA NsG-306-63 progress report for the period 1 January 1967 to 30 June 1967, Aerospace and Mechanical Sciences Rept. No. 634i, July 1967, Princeton Univ., Princeton, N. J.

[55]Clark, K. E. and Jahn, R. G., "The Magnetoplasmadynamic Arc," Astronautica Acta, Vol. 13, No. 4, 1967, pp. 315-325.

[56]Jahn, R. G., "The MPD Arc," NASA Contract NASw-1513, Aug. 1967, Giannini Scientific Corp., Santa Ana, Calif.

[57]Eckbreth, A. C., Clark, K. E. and Jahn, R. G., "Current Pattern Stabilization in Pulsed Plasma Accelerators," A.I.A.A. Bulletin, Vol. 4, No. 9, Sept. 1967, p. 433.

[58]Clark, K. E., Eckbreth, A. C. and Jahn, R. G., "Current Pattern Stabilization in Pulsed Plasma Accelerators," A.I.A.A. Paper 67-656, A.I.A.A. Electric Propulsion and Plasmadynamics Conference, Colorado Springs, Colo., 11-13 Sept. 1967.

[59]Jahn, R. G. and von Jaskowsky, W. F., "Pulsed Electromagnetic Gas Acceleration," NASA NsG-306-63 progress report for the period 1 July 1967 to 31 December 1967, Aerospace and Mechanical Sciences Rept. No. 634j, Jan. 1968, Princeton Univ., Princeton, N. J.

PROJECT REFERENCES

[60]Ducati, A. C., Jahn, R. G., Muehlberger, E. and Treat, R. P., "Exploratory Electromagnetic Thruster Research," TR 117-1513 Annual Report, NASA CR 62047, Feb. 1968, Giannini Scientific Corp., Santa Ana, Calif.

[61]Jahn, R. G., PHYSICS OF ELECTRIC PROPULSION, McGraw-Hill Book Company, New York, 1968.

[62]Burton, R. L. and Jahn, R. G., "Acceleration of Plasma by a Propagating Current Sheet," The Physics of Fluids, Vol. 11, No. 6, June 1968, pp. 1231-1237.

[63]Jahn, R. G. and von Jaskowsky, W. F., "Pulsed Electromagnetic Gas Acceleration," NASA NGR 31-001-005 step-funding renewal proposal for the period 1 October 1968 to 30 September 1971, June 1, 1968, Princeton Univ., Princeton, N. J.

[64]Jahn, R. G. and von Jaskowsky, W. F., "Pulsed Electromagnetic Gas Acceleration," NASA NsG-306/31-001-005 progress report for the period 1 January 1968 to 30 June 1968, Aerospace and Mechanical Sciences Rept. No. 634k, July 1968, Princeton Univ., Princeton, N. J.

[65]Wilbur, P. J., "Energy Transfer from a Pulse Network to a Propagating Current Sheet," Ph.D. thesis, Sept. 1968, Princeton Univ., Princeton, N. J.

[66]Wilbur, P. J. and Jahn, R. G., "Energy Transfer from a Pulse Network to a Propagating Current Sheet," NASA NGR 31-001-005, Aerospace and Mechanical Sciences Rept. No. 846, Sept. 1968, Princeton Univ., Princeton, N. J.

[67]Ducati, A. C., Jahn, R. G., Muehlberger, E. and Treat, R. P., "Exploratory Electromagnetic Thruster Research, Phase II," 2SS108-1513 Interim Report, NASA Contract NASw-1513, Oct. 1968, Giannini Scientific Corp., Santa Ana, Calif.

[68]Eckbreth, A. C., Clark, K. E. and Jahn, R. G., "Current Pattern Stabilization in Pulsed Plasma Accelerators," A.I.A.A. Journal, Vol. 6, No. 11, Nov. 1968, pp. 2125-2132.

PROJECT REFERENCES

[69] Eckbreth, A. C., "Current Pattern and Gas Flow Stabilization in Pulsed Plasma Accelerators," Ph.D. thesis, Dec. 1968, Princeton Univ., Princeton, N. J.

[70] Eckbreth, A. C. and Jahn, R. G., "Current Pattern and Gas Flow Stabilization in Pulsed Plasma Accelerators," NASA NGL 31-001-005, Aerospace and Mechanical Sciences Rept. No. 857, Dec. 1968, Princeton Univ., Princeton, N. J.

[71] York, T. M., "Pressure Distribution in the Structure of a Propagating Current Sheet," Ph.D. thesis, Dec. 1968, Princeton Univ., Princeton, N. J.

[72] York, T. M. and Jahn, R. G., "Pressure Distribution in the Structure of a Propagating Current Sheet," NASA NGL 31-001-005, Aerospace and Mechanical Sciences Rept. No. 853, Dec. 1968, Princeton Univ., Princeton, N. J.

[73] Eckbreth, A. C. and Jahn, R. G., "Current Pattern and Gas Flow Stabilization in Pulsed Plasma Accelerators," A.I.A.A. Bulletin, Vol. 5, No. 12, Dec. 1968, p. 730.

[74] Wilbur, P. J. and Jahn, R. G., "Energy Transfer From a Pulse Network to a Propagating Current Sheet," A.I.A.A. Bulletin, Vol. 5, No. 12, Dec. 1968, p. 730.

[75] Ellis, W. R. and Jahn, R. G., "Ion Density and Current Distributions in a Propagating Current Sheet, Determined by Microwave Reflection Technique," Rept. No. CLM-P-187, Dec. 1968, Culham Laboratory, Abingdon, Berkshire, Great Britain.

[76] Jahn, R. G. and von Jaskowsky, W. F., "Pulsed Electromagnetic Gas Acceleration," NASA NGL 31-001-005 progress report for the period 1 July 1968 to 31 December 1968, Aerospace and Mechanical Sciences Rept. No. 634, Jan. 1969, Princeton Univ., Princeton, N. J.

[77] Eckbreth, A. C. and Jahn, R. G., "Current Pattern and Gas Flow Stabilization in Pulsed Plasma Accelerators," A.I.A.A. Paper 69-112, A.I.A.A. 7th Aerospace Sciences Meeting, New York, N. Y., 20-22 Jan. 1969.

PROJECT REFERENCES

[78]Wilbur, P. J. and Jahn, R. G., "Energy Transfer From a Pulse Network to a Propagating Current Sheet," A.I.A.A. Paper 69-113, A.I.A.A. 7th Aerospace Sciences Meeting, New York, N. Y., 20-22 Jan. 1969.

[79]Ellis, W. R. and Jahn, R. G., "Ion Density and Current Distributions in a Propagating Current Sheet, Determined by Microwave Reflection Technique," Journal of Plasma Physics, Vol. 3, Pt. 2, 1969, pp. 189-213.

[80]York, T. M. and Jahn, R. G., "Pressure Distribution in the Structure of a Propagating Current Sheet," A.I.A.A. Bulletin, Vol. 6, No. 2, Feb. 1969, p. 75.

[81]Clark, K. E. and Jahn, R. G., "Quasi-steady Plasma Acceleration," A.I.A.A. Bulletin, Vol. 6, No. 2, Feb. 1969, p. 75.

[82]York, T. M. and Jahn, R. G., "Pressure Distribution in the Structure of a Propagating Current Sheet," A.I.A.A. Paper 69-264, A.I.A.A. 7th Electric Propulsion Conference, Williamsburg, Va., 3-5 Mar. 1969.

[83]Clark, K. E. and Jahn, R. G., "Quasi-steady Plasma Acceleration," A.I.A.A. Paper 69-267, A.I.A.A. 7th Electric Propulsion Conference, Williamsburg, Va., 3-5 Mar. 1969.

[84]Jahn, R. G. and Mickelsen, W. R., "Electric Propulsion Notebook," A.I.A.A. Professional Study Series, Williamsburg, Va., 1-2 Mar. 1969.

[85]Boyle, M. J., "Plasma Velocity Measurements with Electric Probes," B.S.E. thesis, April 1969, Princeton Univ., Princeton, N. J.

[86]Clark, K. E., "Quasi-steady Plasma Acceleration," Ph.D. thesis, May 1969, Princeton Univ., Princeton, N. J.

[87]Clark, K. E. and Jahn, R. G., "Quasi-steady Plasma Acceleration," NASA NGL 31-001-005, Aerospace and Mechanical Sciences Rept. No. 859, May 1969, Princeton Univ., Princeton, N. J.

PROJECT REFERENCES

[88]Boyle, M. J., "Plasma Velocity Measurements with Electric Probes," Paper No. 4 (Paper presented at the Northeastern Regional Student Conference, Princeton Univ., Princeton, N. J., 9-10 May 1969).

[89]Mickelsen, W. R. and Jahn, R. G., "Status of Electric Propulsion," A.I.A.A. Bulletin, Vol. 6, No. 6, June 1969, p. 257.

[90]Mickelsen, W. R. and Jahn, R. G., "Status of Electric Propulsion," A.I.A.A. Paper 69-497, A.I.A.A. 5th Propulsion Joint Specialist Conference, U. S. Air Force Academy, Colo., 9-13 June 1969.

[91]Ducati, A. C. and Jahn, R. G., "Electron Beam from a Magnetoplasmadynamic Arc," The Physics of Fluids, Vol. 12, No. 6, June 1969, pp. 1177-1181.

[92]Jahn, R. G. and von Jaskowsky, W. F., "Pulsed Electromagnetic Gas Acceleration," NASA NGL 31-001-005 progress report for the period 1 January 1969 to 30 June 1969, Aerospace and Mechanical Sciences Rept. No. 634m, July 1969, Princeton Univ., Princeton, N. J.

[93]Jahn, R. G. and von Jaskowsky, W. F., "Pulsed Electromagnetic Gas Acceleration," NASA NGR 31-001-005 step-funding renewal proposal for the period 1 October 1969 to 30 September 1970, July 1, 1969, Princeton Univ., Princeton, N. J.

[94]Jahn, R. G., Clark, K. E., Oberth, R. C. and Turchi, P. J., "Acceleration Patterns in Quasi-steady MPD Arcs," A.I.A.A. Bulletin, Vol. 6, No. 12, Dec. 1969, p. 701.

[95]Ducati, A. C. and Jahn, R. G., "Repetitively Pulsed, Quasi-steady Vacuum MPD Arc," A.I.A.A. Bulletin, Vol. 6, No. 12, Dec. 1969, p. 701.

[96]Jahn, R. G., von Jaskowsky, W. F. and Clark, K. E., "Pulsed Electromagnetic Gas Acceleration: Acceleration Processes in Quasi-steady Arcs," (Paper delivered at the 6th NASA Intercenter and Contractors Conference on Plasma Physics, NASA Langley Research Center, Hampton, Va., 8-10 Dec. 1969), pp. 8-15.

PROJECT REFERENCES

[97]Jahn, R. G., von Jaskowsky, W. F. and Clark, K. E., "Pulsed Electromagnetic Gas Acceleration," NASA NGL 31-001-005 progress report for the period 1 July 1969 to 31 December 1969, Aerospace and Mechanical Sciences Rept. No. 634n, Jan. 1970, Princeton Univ., Princeton, N. J.

[98]Eckbreth, A. C. and Jahn, R. G., "Current Pattern and Gas Flow Stabilization in Pulsed Plasma Accelerators," A.I.A.A. Journal, Vol. 8, No. 1, Jan. 1970, pp. 138-143.

[99]Jahn, R. G., Clark, K. E., Oberth, R. C. and Turchi, P. J., "Acceleration Patterns in Quasi-steady MPD Arcs," A.I.A.A. Paper 70-165, A.I.A.A. 8th Aerospace Sciences Meeting, New York, N. Y., 19-21 Jan. 1970.

[100]Ducati, A. C. and Jahn, R. G., "Repetitively Pulsed, Quasi-steady Vacuum MPD Arc," A.I.A.A. Paper 70-167, A.I.A.A. 8th Aerospace Sciences Meeting, New York, N. Y., 19-21 Jan. 1970.

[101]Wilbur, P. J. and Jahn, R. G., "Energy Transfer from a Pulse Network to a Propagating Current Sheet," A.I.A.A. Journal, Vol. 8, No. 1, Jan. 1970, pp. 144-149.

[102]Clark, K. E. and Jahn, R. G., "Quasi-steady Plasma Acceleration," A.I.A.A. Journal, Vol. 8, No. 2, Feb. 1970, pp. 216-220.

[103]York, T. M. and Jahn, R. G., "Pressure Distribution in the Structure of a Propagating Current Sheet," The Physics of Fluids, Vol. 13, No. 5, May 1970, pp. 1303-1309.

[104]Jahn, R. G., "Pulsed Electromagnetic Gas Acceleration," NASA NGL 31-001-005 step-funding renewal proposal for period 1 October 1970 to 30 September 1971, June 11, 1970, Princeton Univ., Princeton, N. J.

[105]Jahn, R. G., von Jaskowsky and Clark, K. E., "Pulsed Electromagnetic Gas Acceleration," NASA NGL 31-001-005, progress report for the period 1 January 1970 to 30 June 1970, Aerospace and Mechanical Sciences Rept. No. 634o, July 1970, Princeton Univ., Princeton, N. J.

PROJECT REFERENCES

[106]Turchi, P. J. and Jahn, R. G., "The Cathode Region of a Quasi-steady MPD Arcjet," A.I.A.A. Bulletin, Vol. 7, No. 9, Sept. 1970, p. 449.

[107]Clark, K. E., DiCapua, M. S., Jahn, R. G. and von Jaskowsky, W. F., "Quasi-steady Magnetoplasmadynamic Arc Characteristics," A.I.A.A. Bulletin, Vol. 7, No. 9, Sept. 1970, p. 449.

[108]Turchi, P. J. and Jahn, R. G., "The Cathode Region of a Quasi-steady MPD Arcjet," A.I.A.A. Paper 70-1094, A.I.A.A. 8th Electric Propulsion Conference, Stanford, Calif., 31 Aug.-2 Sept. 1970.

[109]Clark, K. E., DiCapua, M. S., Jahn, R. G. and von Jaskowsky, W. F., "Quasi-steady Magnetoplasmadynamic Arc Characteristics," A.I.A.A Paper 70-1095, A.I.A.A. 8th Electric Propulsion Conference, Stanford, Calif., 31 Aug.-2 Sept. 1970.

[110]Turchi, P. J., "The Cathode Region of a Quasi-steady Magnetoplasmadynamic Arcjet," Ph.D. thesis, Sept. 1970, Princeton Univ., Princeton, N. J.

[111]Turchi, P. J. and Jahn, R. G., "The Cathode Region of a Quasi-steady Magnetoplasmadynamic Arcjet," NASA NGL 31-001-005, Aerospace and Mechanical Sciences Rept. No. 940, Oct. 1970, Princeton Univ., Princeton, N. J.

[112]Oberth, R. C., "Anode Phenomena in High-Current Discharges," Ph.D. thesis, Dec. 1970, Princeton Univ., Princeton, N. J.

[113]Oberth, R. C. and Jahn, R. G., "Anode Phenomena in High-Current Discharges," NASA NGL 31-001-005, Aerospace and Mechanical Sciences Rept. No. 961, Dec. 1970, Princeton Univ., Princeton, N. J.

[114]Di Capua, M. S. and Jahn, R. G., "Voltage-Current Characteristics of Parallel-Plate Plasma Accelerators," A.I.A.A. Bulletin, Vol. 8, No. 1, Jan. 1971, p. 40.

[115]Oberth, R. C. and Jahn, R. G., "Anode Phenomena in High-Current Accelerators," A.I.A.A. Bulletin, Vol. 8, No. 1, Jan. 1971, p. 40.

[116]Di Capua, M. S. and Jahn, R. G., "Energy Deposition in Parallel-Plate Plasma Accelerators," A.I.A.A. Paper 71-197, A.I.A.A. 9th Aerospace Sciences Meeting, New York, N. Y., 25-27 Jan. 1971.

PROJECT REFERENCES

[117]Oberth, R. C. and Jahn, R. G., "Anode Phenomena in High-Current Accelerators," A.I.A.A. Paper 71-198, A.I.A.A. 9th Aerospace Sciences Meeting, New York, N. Y., 25-27 Jan. 1971.

[118]Jahn, R. G., Clark, K. E., Oberth, R. C. and Turchi, P. J., "Acceleration Patterns in Quasi-steady MPD Arcs." A.I.A.A. Journal, Vol. 9, No. 1, Jan. 1971, pp. 167-172.

[119]Jahn, R. G., von Jaskowsky, W. F. and Clark, K. E., "Pulsed Electromagnetic Gas Acceleration," NASA NGL 31-001-005, semi-annual report for period 1 July 1970 to 31 December 1970, Aerospace and Mechanical Sciences Rept. No. 634p, January 1971, Princeton University, Princeton, N. J.

[120]Jahn, R. G., von Jaskowsky, W. F. and Clark, K. E., "Pulsed Electromagnetic Gas Acceleration," NASA NGL 31-001-005 step-funding renewal proposal for the period 1 October 1971 to 30 September 1972, June 16, 1971, Princeton Univ., Princeton, N. J.

[121]Turchi, P. J. and Jahn, R. G., "Cathode Region of a Quasi-steady MPD Arcjet," A.I.A.A. Journal, Vol.9, No. 7, July 1971, pp. 1372-1379.

[122]Clark, K. E., Jahn, R. G. and von Jaskowsky, W. F., "Exhaust Characteristics of a Quasi-steady MPD Accelerator," DGLR Symposium on Electrical Space Thruster Systems, Braunschweig, Germany, June 22-23, 1971.

[123]Cory, J., "Mass, Momentum and Energy Flow from an MPD Accelerator," Ph.D. thesis, Aug. 1971, Princeton Univ., Princeton, N. J.

[124]Di Capua, M. S., "Energy Deposition in the Parallel-Plate Plasma Accelerator," Ph.D. thesis, Princeton Univ., Princeton, N. J., forthcoming.

[125]Bruckner, A. P., Ph.D. thesis, Princeton University, Princeton, N. J., forthcoming.

GENERAL REFERENCES

II-1 Liepmann, H. W. and Roshko, A., Elements of Gasdynamics, John Wiley and Sons, Inc., New York, 1965.

II-2 Jackson, J. D., Classical Electrodynamics, John Wiley and Sons, Inc., New York, 1963.

II-3 Devoto, R. S., "Transport Properties of Partially Ionized Argon," Physics of Fluids, Vol. 10, No. 2, Feb 1967, pp. 354-364.

II-4 Eckert, E. R. G., Heat and Mass Transfer, McGraw-Hill Book Co., Inc., New York, 1959.

III-1 Bohn, W. L., Beth, M.-U., Nedder, G., "On Spectroscopic Measurements of Velocity Profiles and Non-Equilibrium Radial Temperatures in an Argon Plasma Jet," J. Quant. Spectrosc. Radiat. Transfer, Vol. 7, pp. 661-667, 1967, Pergamon Press.

IV-1 Csiky, G. A., "Measurement of Some Properties of a Discharge from a Hollow Cathode," NASA TN D-4966 (Feb. 1969).

IV-2 Byers, D. C. and Snyder, A., "Parametric Investigation of Mercury Hollow Cathode Neutralizer," A.I.A.A. Paper 70-1090, A.I.A.A. 8th Electric Propulsion Conference, Stanford, Calif., 31 Aug.-2 Sept. 1970.

IV-3 Malliaris, A. C., John, R. R., Garrison, R. L. and Libby, D. R., "Quasi-steady MPD propulsion at high power," Final Tech. Rept. AVSD-0146-71-RR, NASA CR-111872, February 1971.

IV-4 Laframboise, J. G., "Theory of Spherical and Cylindrical Langmuir Probes in a Collisionless, Maxwellian Plasma at Rest," Univ. of Toronto Inst. for Aerospace Studies, Rept. No. 100 (1966).

IV-5 Sonin, A. A., "The Behaviour of Free Molecular Cylindrical Langmuir Probes in Supersonic Flows, and their Application to the Study of Blunt Body Stagnation Layer," Univ. of Toronto Inst. for Aerospace Studies, Rept. No. 109 (1965).

Appendix A: Semiannual Statement of Expenditures

PULSED ELECTROMAGNETIC GAS ACCELERATION
NASA NGL 31-001-005

1 January 1971-30 June 1971

Direct Costs			
I.	Salaries and Wages		
	A. Professional	$15,220	
	B. Students	1,556	
	C. Technicians	10,050	
	D. Supporting Staff	5,072	
			$31,898
II.	Employee Benefits (19% of IA, IC, and ID)		5,764
III.	Equipment		0
IV.	Expendable Materials and Services		11,023
V.	Travel		449
VI.	Tuition		1,050
	Total Direct Costs		$50,184
Indirect Costs			
VII.	Overhead (68% of I)		21,690
	TOTAL		$71,874